JPL PUBLICATION 84-81



# Fracture Mechanics Evaluation of GaAs

## Final Report

C.P. Chen

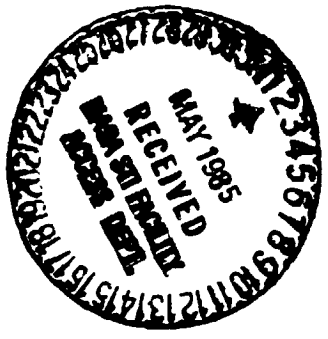


October 15, 1984

Prepared for

**Applied Solar Energy Corporation**

by

**Jet Propulsion Laboratory**
California Institute of Technology
Pasadena, California

TECHNICAL REPORT STANDARD TITLE PAGE

| 1. Report No. 84-81 | 2. Government Accession No. | 3. Recipient's Catalog No. |
|---|---|---|
| 4. Title and Subtitle<br>Fracture Mechanics Evaluation of GaAs | | 5. Report Date<br>October 15, 1984<br>6. Performing Organization Code |
| 7. Author(s)<br>C. P. Chen | | 8. Performing Organization Report No. |
| 9. Performing Organization Name and Address<br>JET PROPULSION LABORATORY<br>California Institute of Technology<br>4800 Oak Grove Drive<br>Pasadena, California 91109 | | 10. Work Unit No.<br>11. Contract or Grant No.<br>NAS7-918<br>13. Type of Report and Period Covered<br>JPL Publication<br>External report |
| 12. Sponsoring Agency Name and Address<br>NATIONAL AERONAUTICS AND SPACE ADMINISTRATION<br>Washington, D.C. 20546 | | 14. Sponsoring Agency Code<br>BZ-055-47-11-06-01 |

15. Supplementary Notes

16. Abstract

The purpose of this work was to generate a data base of mechanical and fracture properties data for single crystal GaAs to be used in the design of reliable GaAs solar cells and modules.

This report contains results of this test program including physical property characterization, fracture behavior evaluation and the strength of cells determined as a function of cell processing and material parameters.

Elastic moduli of GaAs single crystals were found to be highly anisotropic in terms of crystal orientation. The Young's modulus in <111> is 14.4 X $10^{11}$ dyne/cm$^2$ while that in <100> is 8.93 X $10^{11}$ dyne/cm$^2$. The thermal expansion coefficient in the temperature range -130 to 450°C was measured to be 5.5 X $10^{-6}$ m/m °C. No significant variation of the thermal expansion coefficient was found as a function of crystal orientation.

GaAs single crystal was found to be extremely fragile. The minimum fracture toughness of GaAs was measured to be 0.31 MN/m$^{3/2}$ in cleavage on the <110> plane as compared with silicon which has a minimum fracture toughness of 0.82 MN/m$^{3/2}$ in cleavage on the <111> plane. Results suggest that GaAs is susceptible to subcritical crack growth.

Significant changes in fracture strength were found to result from several important processing steps during wafer-to-cell production. The fracture strength data were described by Weibull statistical analysis and can be interpreted in light of the nature of the flaw distribution of the samples.

| 17. Key Words (Selected by Author(s)) | 18. Distribution Statement |
|---|---|
| Conversion Techniques; Electronics and Electrical Engineering; Materials (General); Solid Mechanics | Unclassified; unlimited |

| 19. Security Classif. (of this report) | 20. Security Classif. (of this page) | 21. No. of Pages | 22. Price |
|---|---|---|---|
| Unclassified | Unclassified | | |

JPL 0184 R 9/83

JPL PUBLICATION 84-81

# Fracture Mechanics Evaluation of GaAs

## Final Report

C.P. Chen

October 15, 1984

Prepared for

**Applied Solar Energy Corporation**

by

**Jet Propulsion Laboratory**
California Institute of Technology
Pasadena, California

The research described in this publication was carried out by the Jet Propulsion Laboratory, California Institute of Technology, and was sponsored by the Applied Solar Energy Corporation.

## ABSTRACT

The purpose of this work was to generate a data base of mechanical and fracture properties data for single crystal GaAs to be used in the design of reliable GaAs solar cells and modules.

This report contains results of this test program including physical property characterization, fracture behavior evaluation and the strength of cells determined as a function of cell processing and material parameters.

Elastic moduli of GaAs single crystals were found to be highly anisotropic in terms of crystal orientation. The Young's modulus in <111> is 14.4 X $10^{11}$ dyne/cm$^2$ while that in <100> is 8.93 X $10^{11}$ dyne/cm$^2$. The thermal expansion coefficient in the temperature range -130 to 450°C was measured to be 5.5 X $10^{-6}$ m/m °C. No significant variation of the thermal expansion coefficient was found as a function of crystal orientation.

GaAs single crystal was found to be extremely fragile. The minimum fracture toughness of GaAs was measured to be 0.31 MN/m$^{3/2}$ in cleavage on the {110} plane as compared with silicon which has a minimum fracture toughness of 0.82 MN/m$^{3/2}$ in cleavage on the {111} plane. Results suggest that GaAs is susceptible to subcritical crack growth.

Significant changes in fracture strength were found to result from several important processing steps during wafer-to-cell production. The fracture strength data were described by Weibull statistical analysis and can be interpreted in light of the nature of the flaw distribution of the samples.

## ACKNOWLEDGEMENTS

This work is sponsored by the Applied Solar Energy Corporation (ASEC) under Purchase Order No. 12432, JPL Contract No. 100-00-90-23-16. This support is gratefully acknowledged. Thanks are due to Mr. Ken Ling and Dr. J. Tandon of ASEC for the assistance and encouragement. Thanks also go to Mr. George Datum and Mr. Jim Zumsteg of Lockheed Missiles & Space Company, Inc. for their guidance and support.

Special thanks are extended to many members of the Materials Laboratory Group at JPL, supervised by Mr. Wayne Phillips, for their technical assistance and the experiments, particularly that of Tom Hill and Mark Bronson.

Finally, I would like to thank Dr. Marty Leipold of JPL for his continued interest and direction.

CONTENTS

CONTENTS (continued)

FIGURES

TABLES

Page

## SUMMARY

This report summarizes the work carried out at the Materials Research and Technology Group of the Applied Mechanics Technology Section of the Jet Propulsion Laboratory for the Applied Solar Energy Corporation. The objective of this test program was to generate fundamental data of mechanical properties and fracture behavior of single crystal GaAs. These data are required for design of reliable solar cells and solar panels.

This effort involved single crystal GaAs physical property characterization, fracture behavior evaluation and the strength of solar cells. Solar grade crystalline GaAs doped by Si and Te was evaluated as a function of crystalline orientation and temperature.

Ultrasonic velocity techniques were used to measure Young's modulus and shear modulus while linear dilatometry was utilized to determine the coefficient of thermal expansion of single crystal GaAs in the temperature range -130 to 450°C. The measured elastic moduli of GaAs are summarized in Table A.

Table A. Summary of Measured Elastic Moduli

| Crystal Orientation | Young's Modulus $X10^{11}$ Dyne/cm$^2$ | | Shear Modulus $X10^{11}$ Dyne/cm$^2$ | Poisson's Ratio |
|---|---|---|---|---|
| <100> | 8.93 | | 6.14 | 0.30 |
| <110> | 12.50 | in [001] | 6.14 | |
| | | in [110] | 3.46 | |
| <111> | 14.40 | | 4.35 | |

This result indicated that elastic moduli appear to be highly anisotropic in terms of crystal orientation. The effect of temperature on the elastic modulus was not appreciable in the temperature range -130 to 450°C. No effect of dopant (Si vs Te doped) was observed. The measured coefficient of thermal expansion (CTE) was as follows:

Si doped GaAs = $5.6 \times 10^{-6}$ m/m°C
Te doped GaAs = $5.3 \times 10^{-6}$ m/m°C

The results indicated that no statistically significant variation of measured CTE values as a function of dopant, crystal orientation and temperature (ranging from -130 to 450°C) was found.

Micro-indentation induced flaw techniques were utilized to evaluate the fracture behavior and to determine the fracture toughness of sirgle crystal GaAs in three major crystalline orientations over a range of temperatures. The measured fracture toughness ($K_{IC}$) of GaAs is given in Table B; $K_{IC}$ values of single crystal silicon measured previously are also given in the table for comparison.

Table B. Measured Fracture Toughness, $K_{IC}$ ($MN/m^{3/2}$)

| Crystal Orientation | GaAs | Si |
|---|---|---|
| {100} | 0.43 | 0.95 |
| {110} | 0.31 | 0.90 |
| {111} | 0.45 | 0.82 |

It was found that the minimum fracture toughness of GaAs single crystals occurs in the cleavage plane {110} as compared with silicon having the minimum value in the cleavage plane {111}. In other words, GaAs crystals are extremely fragile and the damage tolerance of GaAs is less than one-half that of silicon single crystals. In addition, no effect of temperature and dopant on the fracture behavior of GaAs was observed. The results also suggest that crystalline GaAs is susceptible to subcritical crack growth.

Fracture strength changes in the in-process wafer-to-cell and items taken at several important stages of the production line were determined. The wafer strength of the cell samples was determined by four-point bending and four-point twisting for 20 X 40 mm rectangular samples and 20 X 20 mm square samples, respectively. The test results for the fracture strength at the 50% fracture probability for as-cut surfaces and polished surfaces as a function of cell processing are summarized in Table C.

Table C. Summary of Fracture Strength of GaAs Solar Cells

Four-point bending-modulus of Rupture (MPa)
at 50% fracture probability.

| Processing | As-Cut Surface | Polished Surface |
|---|---|---|
| Blank Wafer | 57 | 66 |
| MOCVD | 60 | 46 |
| Metallization | 60 | 48 |
| Soldered | 76 | 80 |

Four-point Twisting Fracture Strength (MPa)
at 50% fracture probability

| Processing | Twisting Strength (MPa) |
|---|---|
| Blank Wafer | 75 |
| MOCVD | 79 |
| Metallization | 115 |
| Soldered | 125 |

It was found that mechanical polishing does not produce significant improvement on the strength of the as-cut wafer. MOCVD appears to produce some wafer surface damage which may be the result of thermal shock during vapor deposition. No wafer edge damage was observed as a result of MOCVD.

A preliminary evaluation on the effect of etch pit density on the fracture strength of GaAs wafers was made. The results indicated that the strength of GaAs tends to increase with increasing etch pit density (within the range 5000 to 20,000 EPD/$cm^2$). A more detailed evaluation on the mechanism of defect and alloy hardening in GaAs is required.

SECTION I

## INTRODUCTION

There is increasing interest in the use of crystalline GaAs for photovoltaic and electronic device applications because of its greater conversion efficiency as compared to silicon. However, single crystal GaAs has been found to be extremely fragile. Cracking of GaAs substrates during processing is one of the major sources of solar cell rejection. Cracking of cells in a brittle material like GaAs normally results from the extension of a critical pre-existing flaw under stress. Such flaws, probably generated during ingot slicing, handling and cell processing may therefore control the mechanical strength of solar cells. Due to the presence of pre-existing flaws, the energy required for a crack extension in the material, called fracture toughness, is an important material property controlling the mechanical strength. In order to design a reliable GaAs solar cell, the knowledge of mechanical properties and fracture behavior of material is required. No data is available. In addition, a literature search indicated that even the fundamental physical property data of single crystal GaAs is minimal. No information can be found for GaAs doped by Te and Si for solar cell application.

JPL has developed a unique capability in the area of fracture mechanics evaluation of semiconductor materials, especially for crystalline silicon for solar cells. The data resulting from this testing program has been used by manufacturers of solar cells to enhance production yields, improve cell reliability and durability, and establish mechanical design criteria which has reduced cell cost and has supported development of automated production for the Flat-Plate Solar Array Project.

A program for fracture mechanics evaluation of GaAs sponsored by the Applied Solar Energy Corporation was implemented at JPL in January 1984. The purpose of this report is to present the results obtained

from the test program, which included the following tasks:

1) Physical property characterization,

2) Fracture behavior evaluation, and

3) Strength of cell determination.

The major physical properties of interest are Young's modulus, shear modulus and the coefficient of thermal expansion. The effects of crystalline orientation, dopant and temperature on these physical properties of GaAs are discussed in Section II of this report. A brief description of the fracture behavior program which includes specimen selection and test methods is given. The discussion of test results in terms of the nature of cleavage fracture and measured fracture toughness is presented in Section III. Strength of solar cells, including sample selection, apparatus design and measured results in terms of cell processing steps, is addressed in Section IV. Major conclusions resulting from the conduct of each task of this test program are given in the end of each section. Recommendations for future work are suggested in Section V.

SECTION II

# PHYSICAL PROPERTY CHARACTERIZATION

## A. Objectives

A literature search indicated that very little mechanical and physical property data is available for single crystal GaAs. Physical property data available (Ref. 1) did not specify the type of dopant, the impurity level, crystalline orientations or temperature.

The property data for GaAs required immediately for solar cells design are Young's modulus, shear modulus and the coefficient of thermal expansion as a function of:

(1) Temperature range: -130°C to 450°C
(2) Crystalline orientations: <100>, <110>, <111>
(3) Dopant: Silicon and tellurium

## B. Elastic Moduli

### a. Specimens

The specimens for elastic modulus measurement were machined by the supplier* from single-crystal GaAs ingots into cubes with the desired orientation. The cubic specimens were nominally 15 X 15 X 15mm. The sample surface orientations and the electronic properties of the material provided by the supplier are given in Tables II-1 and II-2. The precise dimensions of each specimen were measured using a micrometer prior to the testings.

---

* M/A-Com Laser Diode, Inc., New Brunswick, N. J. 08901

TABLE II-1

Specimens for Elastic Moduli Measurements,

Si Doped GaAs

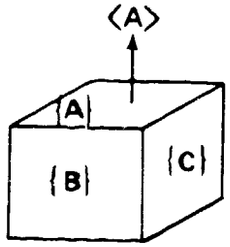


Nominal Dimension = 15 X 15 X 15mm

| Testing Orientation | <100> | <110> | <111> |
|---|---|---|---|
| Surface A | {100} | {110} | {111} |
| Surface B | {110} | {110} | {110} |
| Surface C | {110} | {100} | {211} |
| Crystal No. | 12965 | 13228 | 12965 |
| EPD* ($cm^{-2}$) | 8800 | 3300-6900 | 8800 |
| $\zeta$ (ohm-cm) | 0.0019 | 0.0016-0.0010 | 0.0019 |
| $\mu$ ($cm^2$/volt sec) | 1857 | 1811 - 1563 | 1857 |
| N ($cm^{-3}$) | $1.7 \times 10^{18}$ | $2.1 - 4.0 \times 10^{18}$ | $1.7 \times 10^{18}$ |
| No. of Specimens | 4 | 4 | 4 |

*EPD = etch pit density

$\zeta$ = resistivity

$\mu$ = mobility

N = electron density

Table II-2

Specimens for Elastic Moduli Measurements,

Te Doped GaAs

Nominal Dimension = 15 x 15 x 15 mm

| Testing Orientation | <100> | <110> | <111> |
|---|---|---|---|
| Surface A | {100} | {110} | {111} |
| Surface B | {110} | {110} | {110} |
| Surface C | {110} | {100} | {211} |
| Crystal No. | 12814 | 12813 | 12813 |
| EPD* ($cm^{-2}$) | 6000-6200 | 7100-8800 | 7100-8800 |
| $\zeta$ (Ohm-cm) | 0.0020-0.0011 | 0.0020-0.0014 | 0.0020-0.0014 |
| $\mu$ ($cm^2$/Volt Sec) | 2675-1734 | 2661-1978 | 2661-1978 |
| N ($cm^{-3}$) | 1.2 - $3.3X10^{18}$ | 1.2 - $2.3X10^{18}$ | 1.2-$2.3X10^{18}$ |
| No. of Specimens | 4 | 4 | 4 |

*See Table II-1 for definitions.

b. Test Method

The test method commonly used to determine elastic moduli of solid materials is either mechanical resonance[2,3] or sonic velocity[4-6]. Since single crystal GaAs is expected to be anisotropic as a function of crystalline orientation, sonic velocity measurement by the ultrasonic pulse-echo technique[4-6] was used in this test program.

The testing set-up is shown schematically in Fig. II-1. One transducer was used in the pulse-echo mode to measure the ultrasonic velocity of longitudinal waves while two transducers - one for pulsing and another for receiving - were used to measure the shearing wave velocity. GaAs crystals have greater attenuation of shear waves than longitudinal waves. Lead metaniobate transducers were used for this test because of the temperature range requirements of the test program. The sonic signals were analyzed using an ultrasonic apparatus*. Epoxy cement was utilized to bond the transducer on the GaAs sample for testing from -130°C to 150°C. High temperature cement** was used for temperatures greater than 150°C.

The temperature was controlled by a temperature chamber as shown in Figure II-1. For test temperatures below room temperature, a controlled flow of $LN_2$ vapor was used. A heating element in the test chamber was used for testing above room temperature. The testing temperature was controlled within +5°F (≈3°C).

c. Test Results and Discussion

Ultrasonic velocity measurements were carried out on all 4 specimens of each type provided by the supplier. Since the

* Model No. CL 204, Krautkramer-Branson, Stratford, CN.

** Sauereisen 29B and hardener, Sauereisen Cements Co., Pittsburgh, PA 15238.

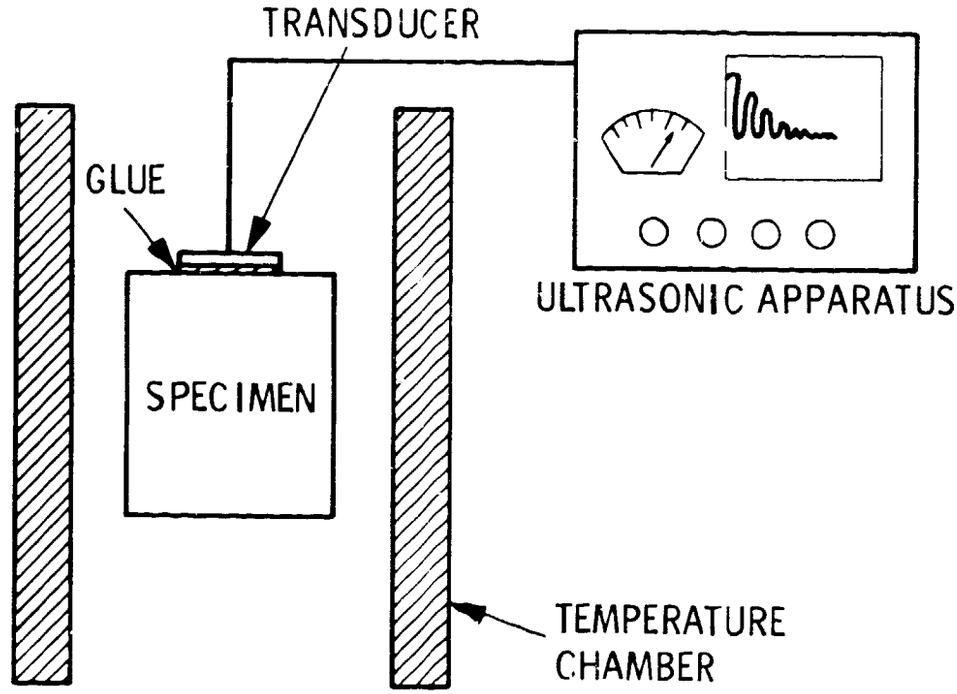


TRANSDUCER = LEAD METANIOBATE
ULTRASONIC APPARATUS = KRAUTKRAMER - BRANSON
MODEL No. CL204
STRATFORD, CN

FREQUENCY = 10 MHz

SAMPLE SIZE = 15 x 15 x 15 mm

Figure II-1. Schematic Showing Ultrasonic Pulse-Echo Technique to Measure Elastic Moduli

atomic packing in <001> and <110> directions on the {110} plane in GaAs are different, shear wave velocities traveling in both <001> and <110> directions on {110} planes were measured. The measured sonic velocities for Si and Te doped GaAs crystals at room temperature are summarized in Tables II-3 and II-4, respectively.

The measured results as shown in Tables II-3 and II-4 are quite consistent in all four specimens. The elastic moduli of Si and Te doped GaAs were then calculated from the average value of the four measured sonic velocities. The relationship between sonic velocity and elastic moduli in crystalline solids is given in References 4-6. The calculated elastic moduli of Si and Te doped GaAs are summarized in Table II-5. Some data reported by Blakemore[1] are also given in Table II-5 for comparison.

As shown in Table II-5, no effect of dopant (Si vs Te doped) on the elastic moduli of GaAs was observed. The measured elastic moduli appear to be highly anisotropic in terms of crystal orientation. For example, the Young's modulus in <111> is 14.40 $\times 10^{11}$ dyne/cm$^2$ while that in <100> is 8.93 $\times 10^{11}$ dyne/cm$^2$. Sonic velocity measurements of GaAs at -130°C indicated no observable change from room temperature data for either longitudinal or shear waves.

The noise in sonic velocity measurements increases with increasing temperature. At 300°C, the noise and pulse distortion became sufficiently profound that the determination of the time between pulses became difficult, especially for shear wave velocity measurement. However, the measured results from ultrasonic velocity in GaAs up to 300°C indicated no appreciable effect. It is anticipated that the elastic moduli of GaAs up to 450°C will not have any significant change from the values at lower temperature. In addition, data reported in Reference 1 on sonic wave velocity in GaAs indicate no appreciable variation from 300°K (Room Temperature) to 77°K (-196°C).

Table II-3
Ultrasonic Measurements on
Si Doped GaAs at Room Temperature

| Crystal # | Wave Propagation Direction | Sample # | Longitudinal Velocity (cm/sec)X10$^5$ | Direction or Plane of Particle Motion | Shear Velocity (cm/sec)X10$^5$ | Density (gm/cm$^3$) |
|---|---|---|---|---|---|---|
| 12965 | <111> | 1 | 5.395 | {111} | 2.84 | 5.310 |
| " | " | 2 | 5.395 | " | 2.85 | 5.312 |
| " | " | 3 | 5.395 | " | 2.84 | 5.311 |
| " | " | 4 | 5.398 | " | 2.91 | 5.311 |
| Average | " | | 5.396 | " | 2.86 | 5.311 |
| | | | | <001> | 3.39 | |
| 13228 | <110> | 1 | 5.237 | <110> | 2.50 | 5.315 |
| | | | | | 3.40 | |
| " | " | 2 | 5.240 | " | 2.51 | 5.311 |
| | | | | | 3.39 | |
| " | " | 3 | 5.237 | " | 2.52 | 5.312 |
| | | | | | 3.39 | |
| " | " | 4 | 5.237 | " | 2.51 | 5.312 |
| | | | | | 3.39 | |
| Average | " | | 5.238 | " | 2.51 | 5.313 |
| 12965 | <100> | 1 | 4.732 | {100} | 3.41 | 5.312 |
| " | " | 2 | 4.732 | " | 3.40 | 5.312 |
| " | " | 3 | 4.732 | " | 3.39 | 5.311 |
| " | " | 4 | 4.732 | " | 3.39 | 5.312 |
| Average | " | | 4.732 | " | 3.40 | 5.312 |

Table II-4
Ultrasonic Measurements on
Te Doped GaAs at Room Temperature

| Crystal # | Wave Propagation Direction | Sample # | Longitudinal Velocity (cm/sec)X10$^5$ | Direction or Plane of Particle Motion | Shear Velocity (cm/sec)X10$^5$ | Density (gm/cm$^3$) |
|---|---|---|---|---|---|---|
| 12813 | <111> | 1 | 5.410 | {111} | 2.85 | 5.316 |
| " | " | 2 | 5.392 | " | 2.84 | 5.316 |
| " | " | 3 | 5.392 | " | 2.85 | 5.316 |
| " | " | 4 | 5.392 | " | 2.84 | 5.314 |
| " | " | | 5.397 | " | 2.85 | 5.316 |
| | | | | <001> | 3.40 | |
| 12813 | <110> | 1 | 5.232 | <110> | 2.51 | 5.319 |
| | | | | | 3.40 | |
| " | " | 2 | 5.232 | " | 2.51 | 5.318 |
| | | | | | 3.41 | |
| " | " | 3 | 5.235 | " | 2.51 | 5.320 |
| | | | | | 3.39 | |
| " | " | 4 | 5.235 | " | 2.51 | 5.318 |
| | | | | | 3.40 | |
| Average | " | | 5.234 | " | 2.51 | 5.319 |
| 12814 | <100> | 1 | 4.732 | {100} | 3.41 | 5.314 |
| " | " | 2 | 4.732 | " | 3.40 | 5.313 |
| " | " | 3 | 4.732 | " | 3.40 | 5.312 |
| " | " | 4 | 4.732 | " | 3.40 | 5.313 |
| Average | " | | 4.732 | " | 3.40 | 5.313 |

TABLE II-5

ELASTIC MODULI OF GaAs

| | Si DOPED | Te DOPED | BLAKEMORE* |
|---|---|---|---|
| YOUNG'S MODULUS ($X10^{11}$ dyne/cm$^2$) | | | |
| $E_{<100>}$ | 8.93 | 8.93 | 8.55 |
| $E_{<110>}$ | 12.50 | 12.50 | |
| $E_{<111>}$ | 14.40 | 14.40 | |
| SHEAR MODULUS ($X10^{11}$ dyne/cm$^2$) | | | |
| $G_{<100>}$ | 6.14 | 6.14 | |
| $G_{<110>}$ in [001] | 6.14 | 6.14 | 3.26** |
| $G_{<110>}$ in [110] | 3.46 | 3.45 | |
| $G_{<111>}$ | 4.35 | 4.34 | |
| POISSON's RATIO | | | |
| <100> | 0.30 | 0.30 | 0.31 |
| DENSITY (gm/cm$^3$) | 5.31 | 5.31 | 5.3173 |

* Ref. 1

** No crystal orientation is given.

It can be concluded that the effect of temperature on the elastic moduli is not appreciable in the testing temperature range (-130 to 450°C) of interest.

C. The Coefficient of Thermal Expansion (CTE)

a. Specimens

The specimens for CTE measurement were small bars, 5 X 6 10mm long, machined by the supplier* into the desired crystalline orientation. The orientations and material properties of each type of specimen provided by the supplier for CTE measurements are given in Tables II-6 and II-7. The precise dimensions of each specimen were measured by a micrometer prior to the testing.

b. Test Method

The coefficient of thermal expansion (CTE) of GaAs at -130°C to 450°C was measured using a dilatometer**. This instrument is shown schematically in Fig. II-2. This instrument can be programmed at any constant heating rate from 0.5°C to 50°C/min. For the GaAs tests, 5°C/min. was used. The measured data were stored on floppy discs and post test analysis performed. The typical curve of linear dimension change as a function of temperature is shown in Fig. II-3. The CTE values can be determined from the slope of any two points of the curve.

c. Test Results and Discussion

As mentioned in the last section, the CTE value at any temperature range can be determined by the slope of the two points of interest on the TMA curve. For small temperature intervals (e.g., $\Delta T$=10°C), CTE values determined had significant

* M/A - Com Laser Diode, Inc., New Brunswick, N. J. 08901.

**Thermomechanical Analyzer (TMA) System, Model 1090/943, DuPont Co., Wilmington, DE 19898.

Table II-6

Specimens for the Coefficient of Thermal Expansion (CTE) Measurements, Si Doped GaAs

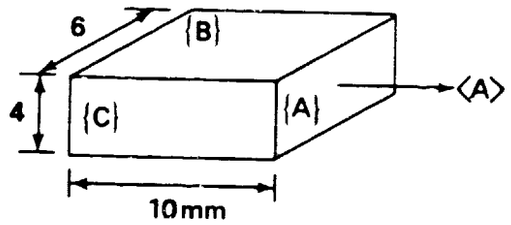


| Testing Orientation | <100> | <110> | <111> |
|---|---|---|---|
| Surface A | {100} | {110} | {111} |
| Surface B | {110} | {110} | {110} |
| Surface C | {110} | {100} | {211} |
| Crystal No. | 12965 | 13228 | 12965 |
| EDP* ($cm^{-2}$) | 9800-8800 | 3300-6900 | 8800 |
| $\varsigma$ (Ohm-cm) | 0.0027-0.0019 | 0.0016-0.0010 | 0.0027-0.0019 |
| $\mu$ ($cm^2$/Volt Sec) | 2380-1857 | 1811-1563 | 2380-1857 |
| N ($cm^{-3}$) | $1.0 - 1.7 \times 10^{18}$ | $2.1 - 4.0 \times 10^{18}$ | $1.0-1.7 \times 10^{18}$ |
| No. of Specimens | 4 | 4 | 4 |

*See Table II-1 for definitions.

Table II-7

Specimens for the Coefficient of Thermal Expansion (CTE) Measurements, Te Doped GaAs

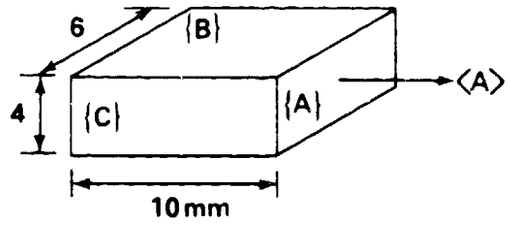


| Testing Orientation | <100> | <110> | <111> |
|---|---|---|---|
| Surface A | {100} | {110} | {111} |
| Surface B | {110} | {110} | {110} |
| Surface C | {110} | {100} | {211} |
| Crystal No. | 12813 | 12813 | 12814 |
| EDP* ($cm^{-2}$) | 7100-8800 | 7100-8800 | 6000-6200 |
| $\zeta$ (Ohm-cm) | 0.0020-0.0014 | 0.0020-0.0014 | 0.0020-0.0011 |
| $\mu$ ($cm^2$/Volt Sec) | 2661-1978 | 2661-1978 | 2675-1734 |
| N ($cm^{-3}$) | $1.2 - 2.3X10^{18}$ | $1.2-2.3X10^{18}$ | $1.2-3.3X10^{16}$ |
| No. of Specimens | 4 | 4 | 4 |

*See Table II-1 for definitions.

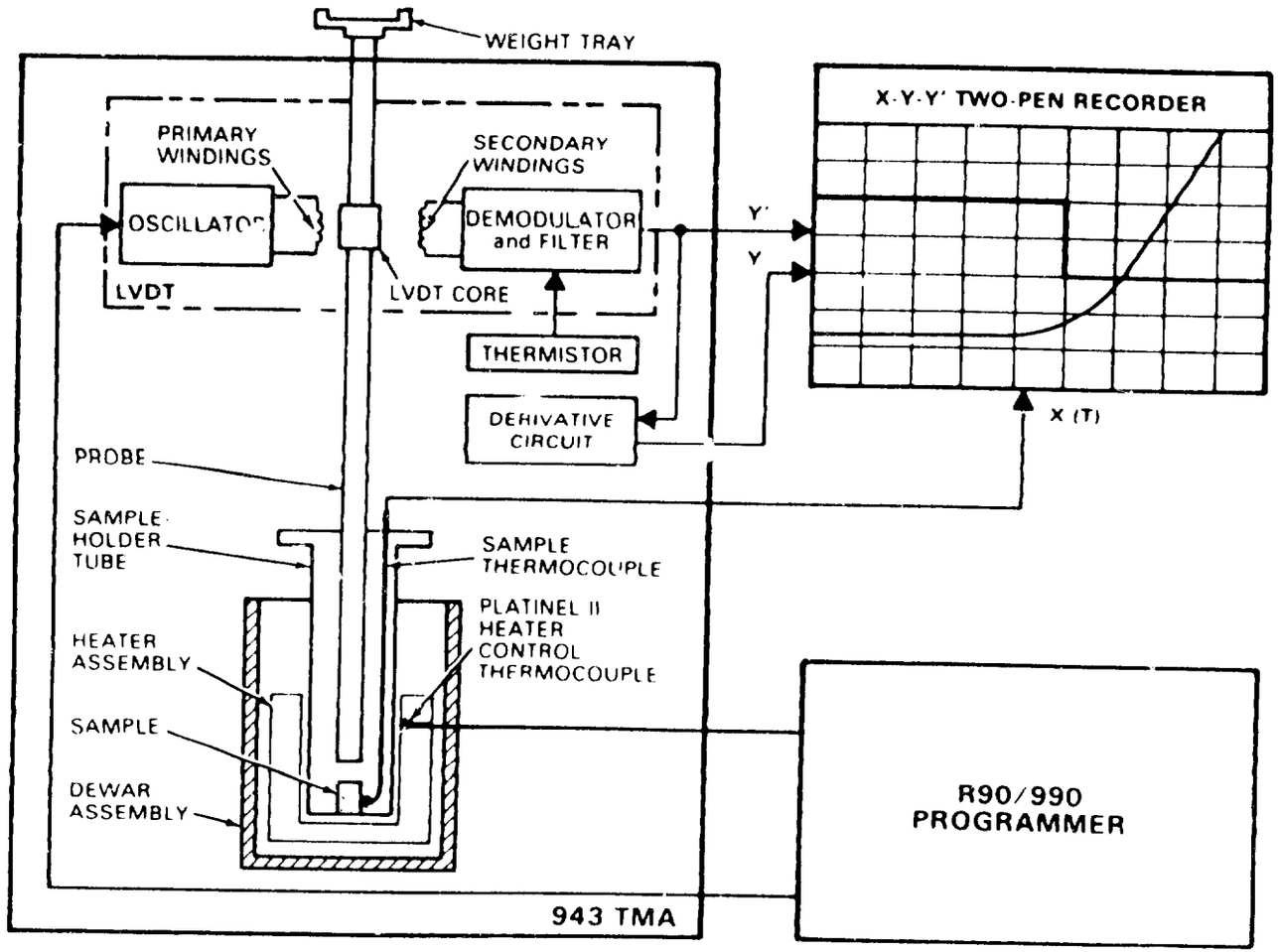


Figure II-2. Diagram Showing DuPont 1090/943 Thermomechanical Analyzer (TMA) System For $\alpha$ Measurement

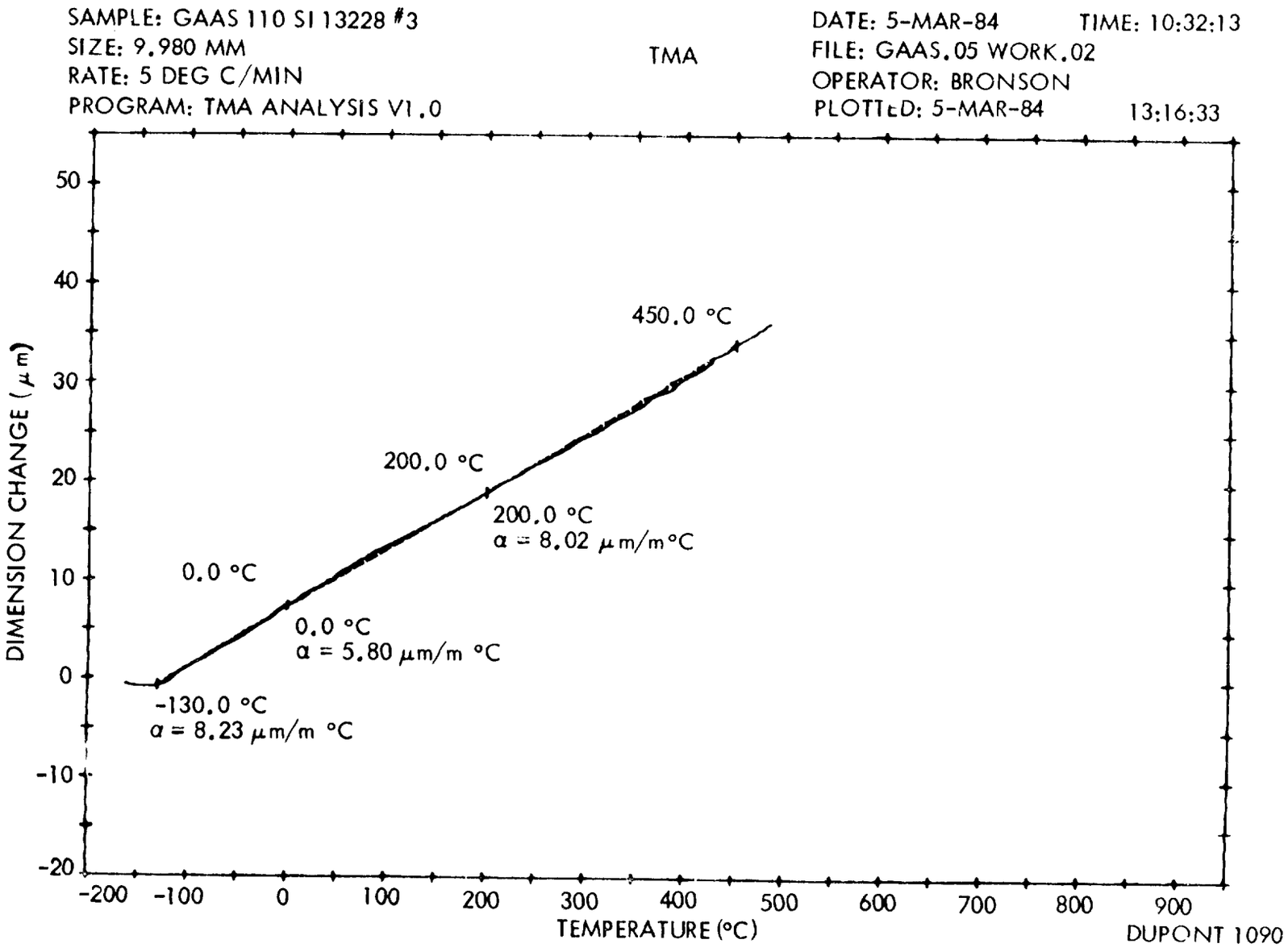


Figure II-3. Typical Curve of TMA Measurement for the Coefficient of Thermal Expansion

scatter. Thus, reasonable CTE values were determined for three temperature ranges: -130°C to 0°C, 0°C to 200°C, and 200 to 450°C, as shown in Fig. II-3. The measured coefficients of thermal expansion (CTE) for these three temperature ranges are presented in Tables II-8 and II-9 for GaAs doped by silicon and tellurium, respectively. It was found that the effect of temperature on the measured CTE values in the temperature range -130°C to 450°C is not statistically significant. In addition, the CTE values were measured in three principal lattice orientations. A very small variation of CTE values as a function of crystal orientation was found. It can be concluded that the CTE values for Si doped and Te doped GaAs crystal are 5.6 X $10^{-6}$ and 5.3 X $10^{-6}$ m/m °C, respectively. The effect of dopant on CTE values is not significant.

## D. CONCLUSIONS

The following conclusions have been drawn from the results of physical property characterization:

1. The elastic moduli of GaAs single crystal were as follows:

| Crystal Orientation | Young's Modulus ($X10^{11}$ Dyne/cm$^2$) | | Shear Modulus ($X10^{11}$ Dyne/cm$^2$) | Poisson's Ratio |
|---|---|---|---|---|
| <100> | 8.93 | | 6.14 | 0.30 |
| <110> | 12.50 | in [001] | 6.14 | |
| | | in [110] | 3.46 | |
| <111> | 14.40 | | 4.35 | |

2. The elastic modulus appears to be highly anisotropic as a function of crystal orientation.

3. No effect of dopant (Si vs Te doped) on the elastic modulus was observed.

TABLE II-8

MEASURED THERMAL EXPANSION COEFFICIENT ($X10^{-6}$ m/m°C)

of GaAs Doped with Silicon

| CRYSTAL ORIENTATION | CRYSTAL No. | SAMPLE No. | TEMPERATURE RANGE -130-0°C | 0-200°C | 200-450°C | Ave. of -130-450°C |
|---|---|---|---|---|---|---|
| <100> | 12965 | 1 | 5.21 | 6.05 | 5.79 | |
| | | 2 | 5.75 | 5.97 | 5.50 | |
| | | 3 | 6.36 | 4.97 | 5.56 | |
| | | 4 | 6.61 | 5.39 | 5.59 | |
| | | Ave | 5.98 | 5.60 | 5.61 | 5.73 |
| | | Std.Dev. | 0.63 | 0.51 | 0.13 | 0.22 |
| <110> | 13228 | 1 | 6.04 | 5.21 | 5.82 | |
| | | 2 | 5.41 | 5.34 | 5.70 | |
| | | 3 | 6.23 | 5.80 | 6.02 | |
| | | 4 | 4.90 | 5.25 | 5.66 | |
| | | Ave | 5.65 | 5.40 | 5.80 | 5.62 |
| | | Std.Dev. | 0.61 | 0.27 | 0.16 | 0.20 |
| <111> | 12965 | 1 | 6.36 | 4.89 | 5.55 | |
| | | 2 | 5.94 | 5.26 | 5.40 | |
| | | 3 | 6.36 | 5.37 | 5.54 | |
| | | 4 | 5.74 | 5.57 | 5.57 | |
| | | Ave | 6.10 | 5.27 | 5.52 | 5.63 |
| | | Std.Dev. | 0.31 | 0.286 | 0.08 | 0.43 |

TABLE II-9

MEASURED THERMAL EXPANSION COEFFICIENT ($X10^{-6}$ m/m°C)

of GaAs Doped with Tellurium

| CRYSTAL ORIENTATION | CRYSTAL No. | SAMPLE No. | TEMPERATURE RANGE -130-0°C | 0-200°C | 200-450°C | Ave. of -130-450°C |
|---|---|---|---|---|---|---|
| <100> | 12813 | 1 | 5.56 | 4.51 | 4.77 | |
| | | 2 | 5.37 | 5.08 | 5.54 | |
| | | 3 | 5.26 | 5.99 | 5.90 | |
| | | 4 | 4.78 | 4.85 | 5.55 | |
| | | Ave | 5.24 | 5.11 | 5.44 | 5.26 |
| | | Std.Dev. | 0.33 | 0.63 | 0.48 | 0.17 |
| <110> | 12813 | 1 | 6.10 | 5.66 | 5.88 | |
| | | 2 | 4.67 | 4.89 | 5.53 | |
| | | 3 | 4.60 | 4.79 | 5.61 | |
| | | 4 | 5.83 | 5.09 | 5.73 | |
| | | Ave | 5.30 | 5.10 | 5.69 | 5.36 |
| | | Std.Dev. | 0.78 | 0.39 | 0.15 | 0.30 |
| <111> | 12814 | 1 | 6.68 | 4.67 | 5.04 | |
| | | 2 | 5.52 | 4.52 | 5.72 | |
| | | 3 | 6.29 | 4.97 | 5.70 | |
| | | 4 | 5.53 | 5.42 | 5.24 | |
| | | Ave | 6.01 | 4.90 | 5.43 | 5.45 |
| | | Std.Dev. | 0.58 | 0.40 | 0.34 | 0.56 |

4. The effect of temperature on the elastic modulus was not significant in the temperature range -130 to 450°C.

5. The measured coefficients of thermal expansion (CTE) in the temperature range -130 to 450°C were:

   Si doped GaAs = $5.6 \times 10^{-6}$ m/m °C
   Te doped GaAs = $5.3 \times 10^{-6}$ m/m °C

   The effect of dopant (Si vs Te) on CTE values is not significant.

6. The effect of temperature on the CTE values within the testing temperature range of -130 to 450°C is not significant.

7. The variation of CTE value as a function of crystal orientation was found to be not statistically significant.

SECTION III

# FRACTURE BEHAVIOR EVALUATION

## A. Objectives

Experience in handling and process ng of single crystal GaAs indicates that GaAs crysta line material is extremely fragile. It fractures by extension of pre-existing flaws in a preferential crystalline plane. This cleavage brittle fracture behavior makes the handling and processing of single crystal GaAs very difficult. It is of great importance to determine the cleavage plane and the damage tolerance of GaAs. No data is available.

One of the most important fracture mechanics damage tolerance parameters for a material is the fracture toughness ($K_{IC}$). This relates to fracture strength, thermal shock resistance, and fatigue fracture. To design GaAs solar cells having mechanical reliability, knowledge of fracture toughness and fracture behavior is necessary.

The purpose of this study was to determine the fracture toughness and to characterize fracture modes of single crystal GaAs as a function of lattice orientations and temperature.

## B. Experimental

### a. Specimens

The specimens were ≈4X6 mm in cross section by 35 mm long. The surfaces of each specimen were in the as-cut condition when they were received from the supplier. The tested surface of each specimen was polished through 600-grit SiC abrasive slurry and then chemically polished* prior to the Vickers indentation and fracture test. The dimensions of each test sample were measured individually by a micrometer. The sample

* Etching solution = $3H_2SO_4$ : 1 $H_2O_2$ : 1 $H_2O$ by volume

surface orientations and the properties of the materials provided by the supplier are given in Tables III-1 and III-2.

b. Test Method

Specimens were tested to fracture under four-point bending to measure the fracture toughness and fracture behavior of GaAs in air at several temperatures. A controlled flaw [7-8] was produced by Vickers diamond indentation at the center of the tensile surface and in the test crystalline plane such that the diagonal of the Vickers pyramid was oriented perpendicularly to the longitudinal axis of the bend bar. Figure III-1 shows the schematic of the cross section of the indented cracks in depth in a bar specimen. The flaw dimensions (a and 2c) of each specimen were measured by a scanning electron microscope at right angles to the fracture surface. A Vickers indentor load at 1000 gm was used to produce a properly controlled flaw.

For a semielliptical surface crack in bending, the Mode I stress intensity factor, $K_{IC}$, is given [7-8] by

$$K_{IC} = \sigma M_B ( \pi a / Q )^{\frac{1}{2}}$$

where $\sigma$ is the maximum outer-fiber tensile stress, $M_B$ is the elastic stress intensity magnification factor, and Q is the flaw shape parameter. Determination of these parameters for brittle materials has been described elsewhere[7-8].

In this study, $K_{IC}$ was measured in the {111}, {110}, and {100} orientations of single-crystal GaAs at -87°C (-125°F), room temperature (≈70°F) and 121°C (250°F). The temperature testing set-up is shown in Fig. III-2. The effect of dopant (Te vs Si doped) on $K_{IC}$ of GaAs is also evaluated. Fifteen (15) samples of each orientation of each type of dopant were available. Thus, 8-9 samples of each orientation were used to test in room temperature and 3 samples each were tested at high and low temperatures.

Table III-1

Specimens for Fracture Toughness Measurements,

Si Doped GaAs

Nominal Dimension = 4 X 6 X 35 mm

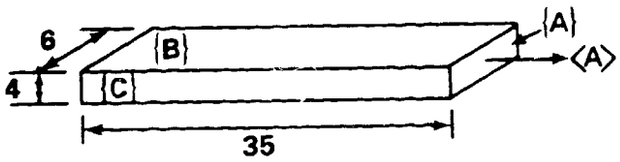


| Testing Orientation | <100> | <110> | <111> |
|---|---|---|---|
| Surface A | {100} | {110} | {111} |
| Surface B | {110} | {110} | {110} |
| Surface C | {110} | {100} | {211} |
| Crystal No. | 13686 | 13566 | 13566 |
| EPD* ($cm^{-2}$) | 8800-19800 | 12,400-20,000 | 12,400-20,000 |
| $\zeta$ (Ohm-cm) | 0.0057-0.0027 | 0.0036-0.0021 | 0.0036-0.0021 |
| $\mu$ ($Cm^2$/Volt Sec) | 2983-2260 | 2746-2091 | 2746-2091 |
| N ($cm^{-3}$) | $0.37\text{-}1.0X10^{18}$ | $0.64\text{-}1.4X10^{18}$ | $0.64\text{-}1.4X10^{18}$ |
| No. of Samples | 15 | 15 | 15 |

*See Table II-1 for definitions.

Table III-2

Specimens for Fracture Toughness Measurements,

Te Doped GaAs

Nominal Dimension = 4 X 6 X 35 mm

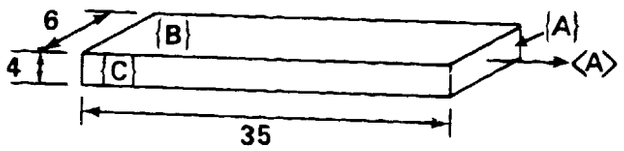


| Testing Orientation | <100> | <110> | <111> |
|---|---|---|---|
| Surface A | {100} | {110} | {111} |
| Surface B | {110} | {110} | {110} |
| Surface C | {110} | {100} | {211} |
| Crystal No. | 13381 | 12814 | 13373 |
| EPD* ($cm^{-2}$) | 6400-7800 | 6000-6200 | 7100-5400 |
| $\zeta$ (Ohm-cm) | 0.0042-0.0022 | 0.0020-0.0011 | 0.0029-0.0016 |
| $\mu$ ($cm^2$/Volt Sec) | 2324-2242 | 2675-1734 | 2942-2207 |
| N ($cm^{-3}$) | $0.64\text{-}1.2\text{X}10^{18}$ | $1.2\text{-}3.33\text{X}10^{18}$ | $1.0\text{-}1.8\text{X}10^{18}$ |
| No. of Samples | 15 | 15 | 15 |

*See Table II-1 for definitions.

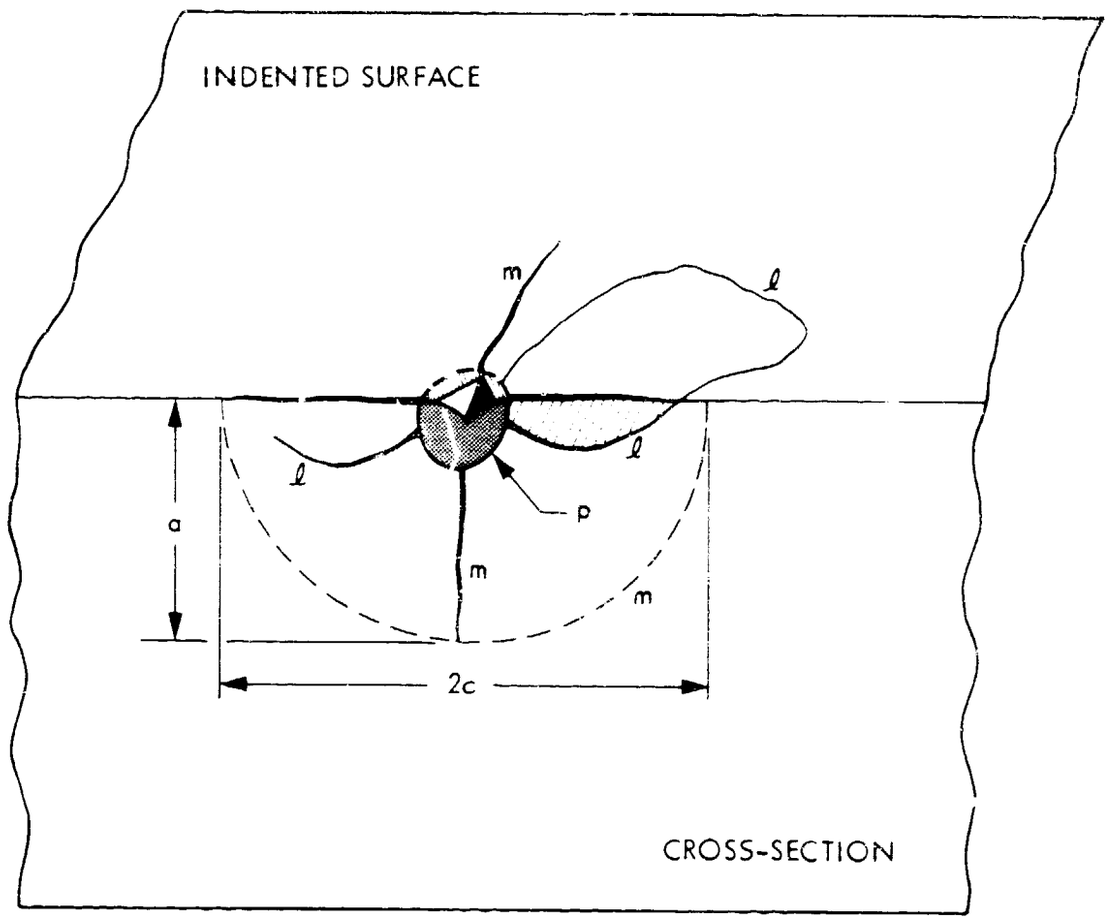


Figure III-1. Schematic Showing the Cross-Section of Vickers Indented Cracks in a GaAs Bar Specimen (m = Median/Radial Cracks; ℓ = Lateral Crack; p = Plastic Deformed Zone)

Figure III-2. $K_{IC}$ Test Fixture in Temperature Chamber

C. Test Results and Discussion

a. Fracture Toughness ($K_{IC}$)

The measured fracture toughness ($K_{IC}$) data of GaAs at room temperature is summarized in Table III-3. No change in $K_{IC}$ values as a function of dopant was found. The $K_{IC}$ values in Table III-3 are the average of 15 to 18 tests including both Si and Te doped GaAs. The effect of temperature (-87°C to 121°C) on $K_{IC}$ was also evaluated. The measured $K_{IC}$ data at high and low temperatures are within the scatter of the room temperature data. These data can be expected within the temperature range -87 to 121°C.

As shown in Table III-3, the minimum $K_{IC}$ value was found in {110} plane which suggested that {110} plane is the easy cleavage plane of single crystal GaAs. The $K_{IC}$ value in the {110} cleavage plane was measured to be 0.31 $MNm^{-3/2}$. It should be noted that the minimum $K_{IC}$ of single crystal silicon measured[8] by the same technique was 0.82 $MNm^{-3/2}$ and cleaved in {111} planes. In other words, GaAs crystals are extremely fragile and the damage tolerance of GaAs is less than one-half that of silicon single crystals.

b. Fracture Surfaces:

{100} Fracture:

A typical Vickers indentation on the surface of a <100> sample is shown in Fig. III-3(a), in which the median cracks and a lateral crack are seen. The orientation of the median cracks is shown in Fig. III-3(b). A typical {100} fracture of single crystal GaAs is shown in Fig. III-3(c). A higher magnification photo near the fracture originating flaw is shown in Fig. III-3(d). When a <100> bar was subjected to a <100> bending moment, the flaw initially extended for a small distance on the {100} plane both sideways and in depth from the tensile surface. It then proceeded along multiple {110} planes.

TABLE III-3

MEASURED $K_{IC}$ OF GaAs AT ROOM TEMPERATURE

CONTROLLED FLAW BY 1000 gm VICKERS

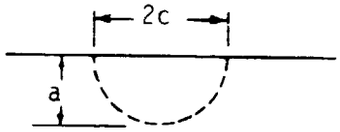


| Crystal Orientation | 2c (μm) | a (μm) | $K_{IC}$ ($MNm^{-3/2}$) | ($K_{IC}$ of Si*) ($MNm^{-3/2}$) |
|---|---|---|---|---|
| {100} | 354±38 | 144±20 | 0.43±0.031 | 0.95 |
| {110} | 264±35 | 131±25 | 0.31±0.030 | 0.90 |
| {111} | 307±67 | 150±10 | 0.45±0.025 | 0.82 |

*Chen and Leipold, 1980 (Ref. 8)

(a)

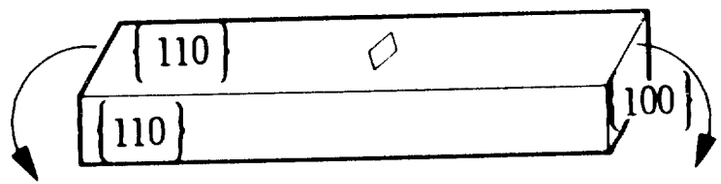


(b)

(c)

(d)

Figure III-3. Typical Fracture of <100> Sample

{110} Fracture:

A typical Vickers indentation on the surface of a <110> sample is shown in Fig. III-4(a) and the orientation of the median cracks is indicated in Fig. III-4(b). The typical fracture surface and the fracture originating flaw on the {110} plane of single crystal GaAs are shown in Fig. II-4(c) and (d), respectively. It can be seen that the fracture originating flaw is approximately semicircular and that the crack extension is entirely on the {110} plane of the specimen. The {110} plane appears to be the cleavage plane of single crystal GaAs. It is reported[8] that the cleavage plane of single crystal silicon is the {111} plane.

{111} Fracture:

A typical Vickers indentation on the surface of a <111> sample is shown in Fig. III-5(a). The orientation of the <111> sample is given in Fig. III-5(b). The median cracks as seen in Fig. III-5(a) are not parallel to {111}. In other words, the fracture-originating flaws are not in the {111} plane. When a <111> bar was subjected to a <111> bending moment, cracks tended to propagate on the planes at an angle approximately 35° to the {111} plane. The typical fracture surface and the fracture originating flaw are shown in Fig. III-5(c) and (d), respectively. Evaluation of the fracture surfaces of the tested <111> samples indicated that the crack propagation of <111> samples is on the {110} planes. Therefore, the fracture of the <111> bar is mixed mode I, tensile fracture, and II, shear fracture.

It should be noted that lateral cracks were usually found at the Vickers indentation on the surface of testing samples, such as shown in Fig. III-3(a) and III-4(a). During the Vickers

(a)

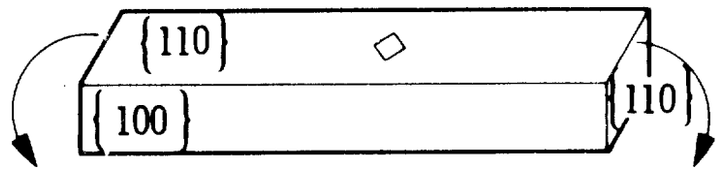


(b)

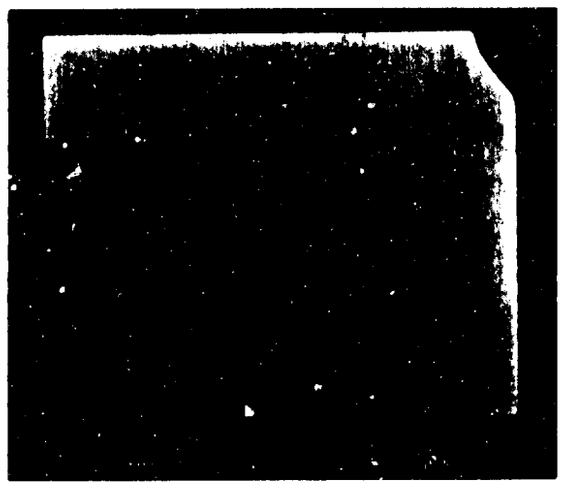

(c)

(d)

Figure III-4. Typical Fracture of <110> Sample

(a)

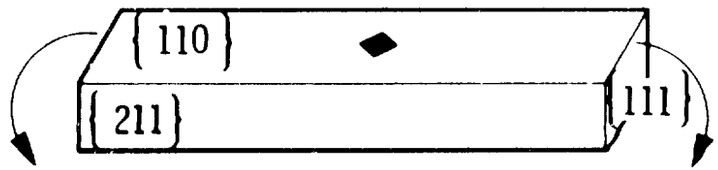


(b)

(c)

(d)

Figure III-5. Typical Fracture of <111> Sample

microindentation test, the indent on the sample surface was examined by a microscope after the indentor was removed. In many cases, lateral cracks popped out during the microscope examination. This delayed cracking suggests that GaAs is susceptible to subcritical crack growth. The subcritical crack growth property of GaAs is of great importance because the fracture of GaAs solar cells in field service can result from subcritical crack growth. Subcritical crack growth in GaAs may be monitored by an acoustic emission technique[11].

## D. CONCLUSIONS

1. The minimum fracture toughness of GaAs was measured to be 0.31 $MNm^{-3/2}$ in cleavage plane {110} as compared with single crystal silicon which has a minimum fracture toughness of 0.82 $MNm^{-3/2}$ with cleavage in {111}.

2. No effect of Te versus Si doping on the fracture toughness of GaAs was observed.

3. No effect of temperature (-87°C to 121°C) on the $K_{IC}$ value of GaAs was observed.

4. Results suggest that crystalline GaAs is susceptible to subcritical crack growth.

SECTION IV

# STRENGTH OF GaAs SOLAR CELLS

## A. Objectives

The objective was to evaluate cell cracking characteristics and changes in fracture strength of GaAs solar cells in a present state-of-the-art of manufacturing process for GaAs solar cells from wafer to complete cell of a typical production line. Several key cell production process steps were identified. The fracture strength of cells at these processing steps at several temperatures was evaluated. The effect of etch pit density (EPD) on the strength of GaAs wafers was determined. The test specimens, test methods and test results are described in the following pages.

## B. Experimental

### a. Specimens

The test specimens were single crystal GaAs wafers, approximately 0.3 mm in thickness, 20 X 20 mm and 20 X 40 mm nominal dimension. They were supplied by a solar cell manufacturer* as a series of blank wafers and cell samples taken at several process steps as follows:

(1) Blank wafers - one surface was as-polished (polished mechanically and chemically) and another surface was in as-cut condition (with light chemical polishing). The edges of the wafer are in as-cut condition (no edge rounding).

---

* Applied Solar Energy Corp., City of Industry, CA.

(2) MOCVD - MOCVD was applied on the polished surface. The as-cut surface was uncoated.

(3) Metallization - Metal grid was applied on the MOCVD surface and the metal back contact was made on the as-cut surface.

(4) Soldered - solder was applied on the metal backing surface as well as on the grid. On the grid surface of the solar cell, an anti-reflection (AR) coating was then applied. The surface conditions of these two surfaces of the wafer samples at each processing step are summarized in Table IV-..

Table IV-1

Surface Condition Changes after each Processing Step

| Process Step | Polished Surface | As-Cut Surface |
|---|---|---|
| Blank Wafer | as-polished | as-cut with light chemical polishing |
| MOCVD | MOCVD | unchanged |
| Metallization | Metal Grids | Metal Back Contact |
| Soldered | Solder on grids and AR coating | Soldered |

The properties of the GaAs material were as follows:

Orientation = 2° off <100>
Dopant = Si
Resistivity Range, $\zeta$ = 0.0018-0.011 Ω-cm
Electron density, N = $2.0 \times 10^{18} - 4.5 \times 10^{18}/cm^3$
Etch Pit Density (EPD) = ≈10,000/$cm^2$

In addition, blank wafers only with EPD values 5000/cm$^2$ and 20,000/cm$^2$ in both sizes = 20 X 20 mm and 20 X 40 mm were evaluated.

b. Test Methods

The mechanical strength of single crystal GaAs wafers and cells was evaluated by four-point bending for 20 X 40 mm rectangular samples and four-point twisting for 20 x 20 mm square samples. The four-point bending test jig is shown in Fig. IV-1(a) and the dimensions of the test jig are given schematically in Fig. IV-1(b). The modulus of rupture of GaAs wafers was calculated from the equation:

$$\sigma = 24 \times 10^{-3} \frac{P}{W t^2} \quad \text{(Newton)} \qquad \text{(IV-1)}$$

where P = fracture force, W & t = dimensions of sample; see Fig. IV-1(b).

The four-point twisting test jig is shown in Fig. IV-2(a). Using this test method, a wafer sample is loaded as shown in Fig. IV-2(b) or (c). The strength of the wafer is:

$$\sigma = \frac{3}{2\sqrt{2}} \frac{P d}{L t^2} \quad \text{loaded at corners} \qquad \text{(IV-2)}$$

$$\sigma = \frac{3}{2} \frac{P d}{L t^2} \quad \text{loaded at edges} \qquad \text{(IV-3)}$$

where L & t = dimensions of samples see Fig. IV-2(b) and (c),

d = diameter of 4-point loading points. In this test, d = 19.2 X 10$^{-3}$ m

The four-point bending test and the four-point twisting test were discussed in detail in Ref. 9. The four-point bending method stresses only portions of the sample, while four-point twisting stresses the entire wafer including edges and internal area. For a small sample under four-point twisting, the edge crack extension is the controlling factor for the fracture of a square GaAs sample, since the transverse shear stresses at the edges are maximum.

Figure IV-1. Four-Point Bending Test for 20 x 40 mm Samples

Figure IV-2. Four-Point Twisting Test for 20 x 20 mm Samples

The strength of 20 X 20 mm and 20 X 40 mm samples was tested at room temperature in air. However, a small number of 20 X 40 mm samples at several processing stages were tested at -87°C and 121°C to determine the effect of temperature on the strength of GaAs cells. These temperatures were chosen based on the extremes of the temperature which a GaAs cell may experience in field service and quality assurance testing.

## C. Test Results and Discussion

Strength data resulting from studies of brittle materials typically show a great deal of scatter. For this reason the conventional method of representing observed quantities using the arithmetic mean and its standard deviation may not show a meaningful characteristic of strength distribution. A statistical method commonly used to describe the strength of brittle materials is that given by Weibull[10]. According to this method, a formula of the form given below is used to relate the probability of failure, G, with stress, S.

$$G = 1 - \exp\left[-\int_V \left(\frac{S - S_u}{S_o}\right)^m dV\right]$$

where $S_u$ is the stress below which none of the samples will fail, $S_o$ is a normalizing factor, m is termed the Weibull modulus, and V is the volume of material under uniaxial stress where fracture initiates. $S_u$, $S_o$ and m are material properties and are called Weibull parameters. In Weibull analysis it is assumed that fracture at the most critical flaw under a given stress distribution leads to total failure. Thus, the Weibull method is also called "Weakest Link Statistics".

For material under bending, the critical flaw which causes fracture is most often on the surface. Thus, the fracture probability, G, for material under bending can be expressed as a function of surface area, A:

$$G = 1 - \exp\left[-\int_A \left(\frac{S - S_u}{S_o}\right)^m dA\right]$$

From this equation it is apparent that the larger the surface area of the material under bending stress, the lower the strength distribution obtained from the test. This phenomenon can be interpreted to mean that the larger the surface area under stress, the greater the probability of finding a larger flaw. Therefore, strength data of brittle material depends on both the test sample size and the extent to which the test method stresses all of the surface area of the sample.

The typical Weibull plot to describe strength data of brittle material is shown in Figure IV-3. The strength distribution of this Weibull plot can also be described by the distribution of the critical flaw size in the samples. The larger flaw size is found in the fractured sample at the left-hand side (lower strength) of the curve, while the smaller flaw size is at the right-hand side of the curve.

It is important to note that the Weibull modulus, m, which describes the slope of the curve, is related to the flaw size distribution of a material. The smaller m value indicates greater distribution of sizes of flaws, greater scatter of the strength data, and shows a lower slope on the Weibull curve. The Weibull plot will be used to display and interpret the general characteristics of strength data on GaAs solar cells for both 20 X 40 mm samples tested by four-point bending and 20 X 20 mm samples tested by four-point twisting method.

a. Effect of Cell Processing

Since the GaAs solar cells are manufactured from wafers which have one surface polished both mechanically and chemically, and the other surface is in as-cut condition and etched chemically,

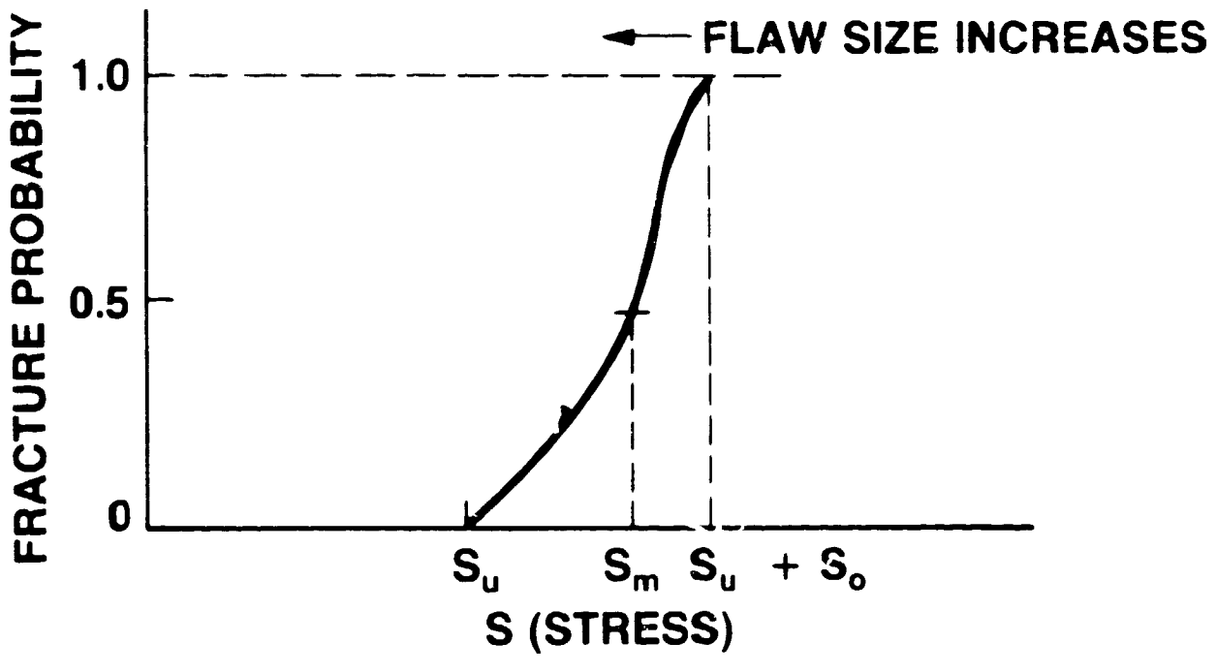


$$\text{FRACTURE PROBABILITY} = 1 - \exp\left[-\int_v \left(\frac{S - S_u}{S_o}\right)^m dV\right]$$

| | | |
|---|---|---|
| $S_u$ | = | STRESS BELOW WHICH NONE WILL FAIL |
| $S_u + S_o$ | = | STRESS ABOVE WHICH ALL WILL FAIL |
| $S$ | = | STRESS OF INTEREST |
| $m$ | = | WEIBULL MODULUS (RELATE TO SLOPE OF PLOT) |
| $S_m$ | = | S AT 0.5 G, $S_m \approx S_{AVE}$ |

Figure IV-3. Data Analysis Method - Weibull Statistic

the effect of cell processing on the strength of each surface was evaluated, and then a comparison of the changes of the strength of these two surfaces after each processing step was made.

The effect of cell processing on the strength of the polished surface of 20 X 40 mm cells tested by four-point bending at room temperature is shown in Fig. IV-4, plotted in Weibull statistical distribution. As shown in Fig. IV-4, the strength at 50% fracture probability of the polished surface of blank wafers is approximately 66 MPa as compared with that of the same surface after MOCVD (≈46MPa). The strength of wafers after MOCVD has decreased appreciably. This strength degradation may have resulted from flaw extension induced by thermal stresses during MOCVD processing. The effect of thermal stresses on the strength of GaAs is of great interest. The statistical distribution indicated that no change in strength of the metal grid surface after metallization from MOCVD was observed. However, the application of the soldering metal layer and AR coating on the grid surface of a cell gave a significant increase in the measured bending strength. The strength at 50% fracture probability of a complete cell after soldering is ≈80MPa.

The effect of cell processing on the strength of the as-cut surface of 20 X 40 mm cells tested at room temperature is shown in Fig. IV-5. Only 5 samples for each step of cell processing were available for the test. The determination of the effect of cell processing was difficult by any statistical means. However, Fig. IV-5 indicated that the strength of soldered cells appears to be greater than the blank wafers. The strength at 50% fracture probability for the as-cut surface of blank wafers is approximately 57 MPa compared with ≈76 MPa for soldered cells.

A comparison of the strength of as-polished and as-cut surfaces of wafers at several processing steps was made as shown in Fig. IV-6 to IV-8. Fig. IV-6 shows the room temperature strengths at 50% fracture probability for as-cut and as-polished

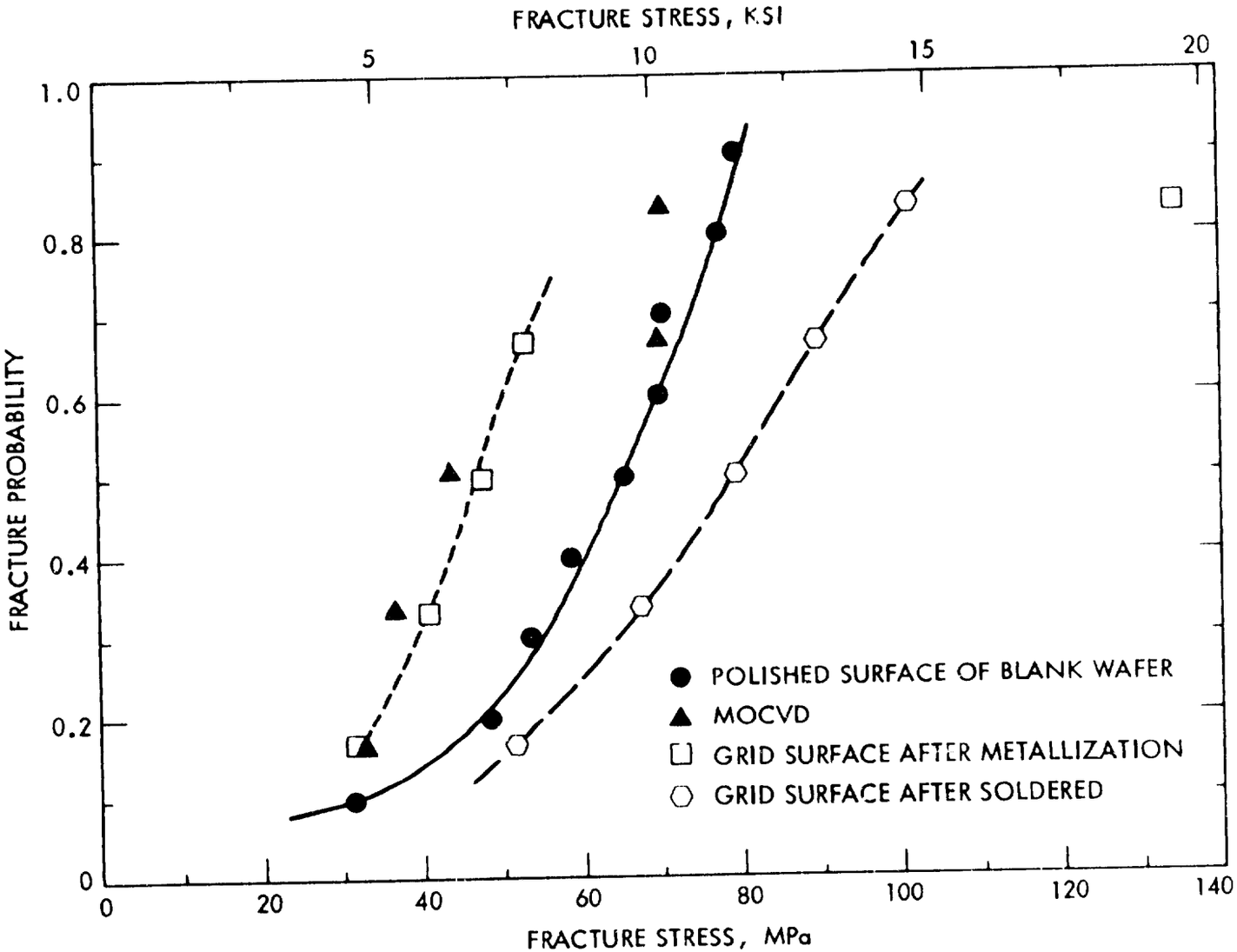


Figure IV-4. Effect of Cell Processing on the Modulus of Rupture of Polished Surface of 2 x 4 cm Cells Tested at Room Temperature, Weibull Statistical Distribution Plot

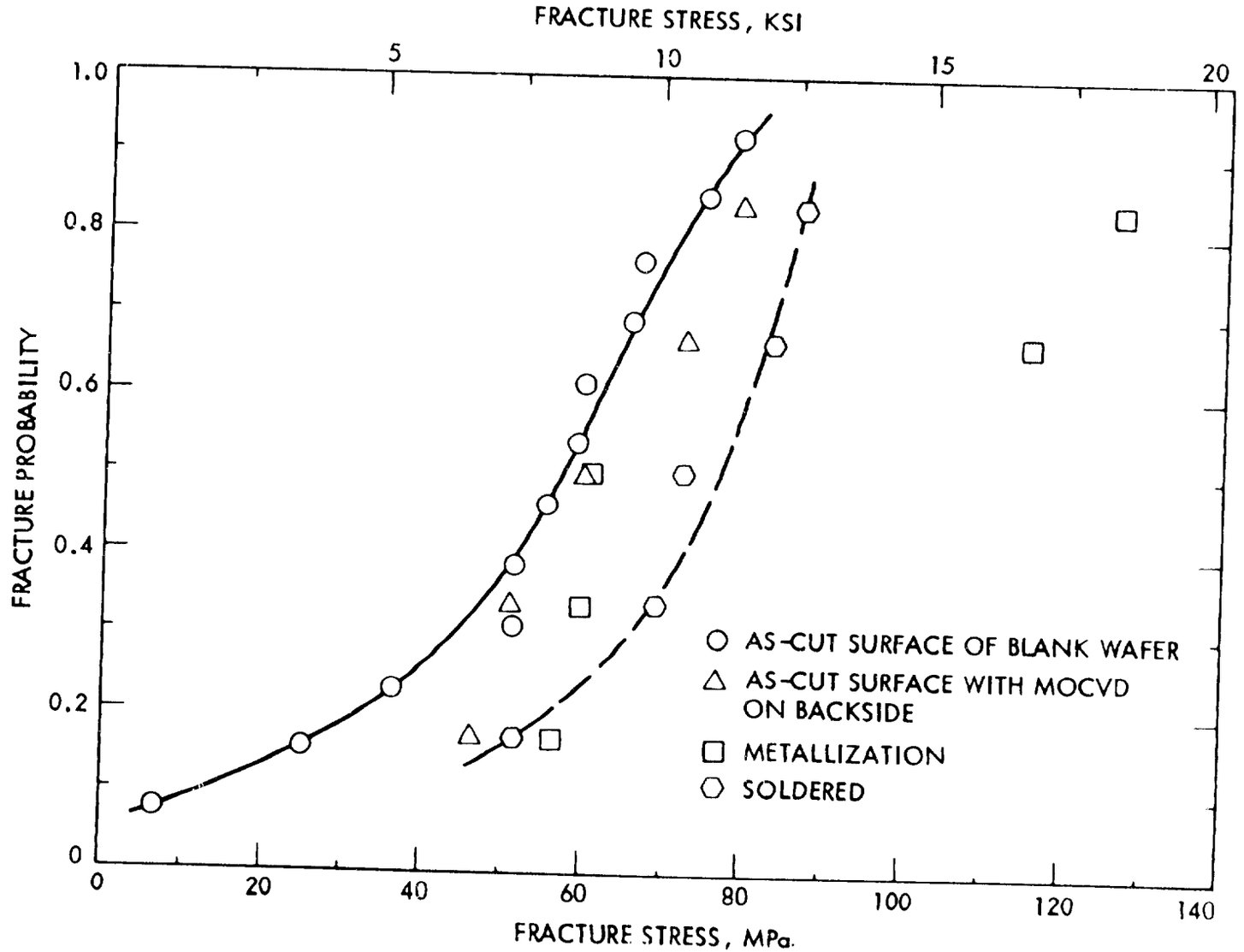


Figure IV-5. Effect of Cell Processing on the Modulus of Rupture of As-Cut Surface of 2 x 4 cm Cells Tested at Room Temperature, Weibull Statistical Distribution Plot

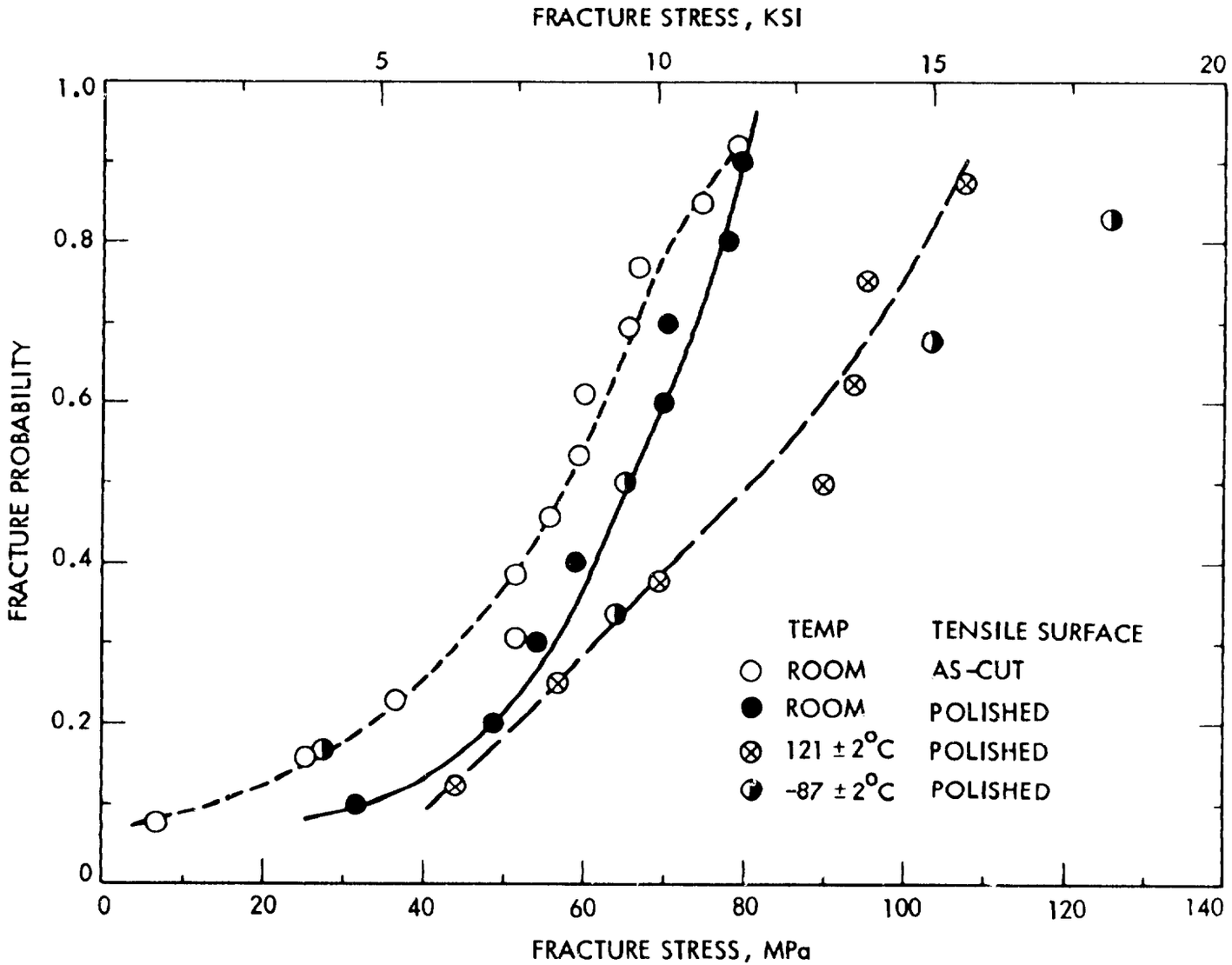


Figure IV-6. Effect of Temperature on the Modulus of Rupture of GaAs 2 x 4 cm Blank Wafer, Weibull Statistical Distribution Plot

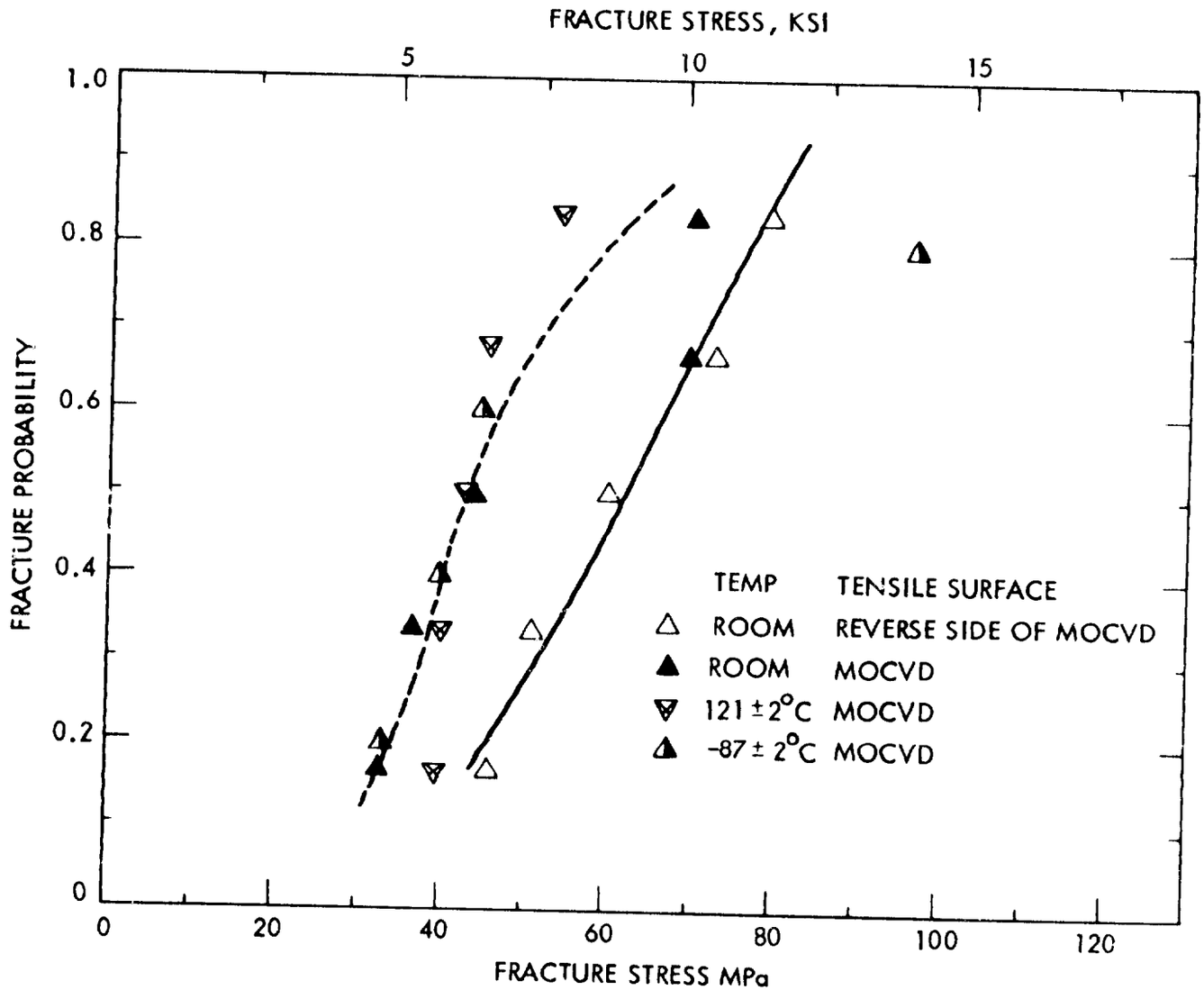


Figure IV-7. Effect of Temperature on the Modulus of Rupture of GaAs 2 x 4 cm Wafer After MOCVD, Weibull Statistical Distribution Plot

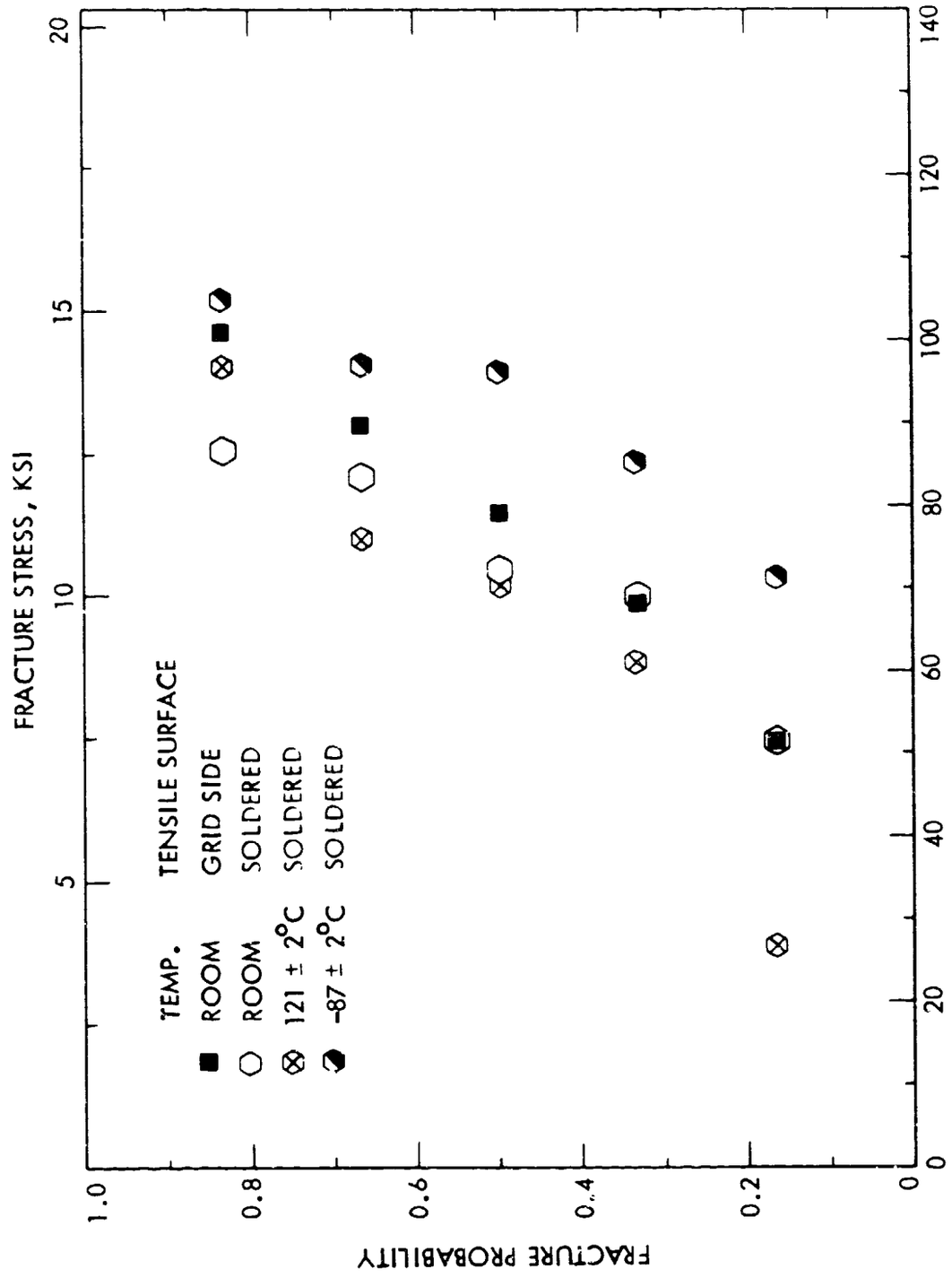


Figure IV-8. Effect of Temperature on the Modulus of Rupture of GaAs 2 x 4 cm Solar Cell After Soldered, Weibull Statistical Distribution Plot

surfaces of blank wafers are 57 MPa and 66 MPa, respectively. As mentioned before, the as-polished surfaces of the wafer samples were polished by both mechanical and chemical methods while as-cut surfaces of the blank wafers were polished chemically. Approximately 13% increase in strength resulted from mechanical polishing. From the curves of as-cut and as-polished wafer strengths in Fig. IV-6, the mechanical polishing was shown to reduce the surface flaw size at the large flaw size ends of the distribution curves. Mechanical polishing, however, has no effect on the small size ends of the distribution curves. Both curves reveal a long tail at the low-stress portion. The wafers in the low-strength distribution are likely to be fractured during subsequent cell processing and handling. Such failures result in costs associated with earlier processing and potential destruction of other good wafers. The strength distribution curves of as-cut and as-polished wafers suggest that the mechanical polishing cannot effectively eliminate those weak samples; a proof testing would be desirable to eliminate those weak samples before the subsequent cracking occurs. Mechanical proof testing[12] has been shown to be useful to eliminate weak samples in cell processing and to evaluate crack growth during proof testing. The effect of MOCVD on the strength of the as-cut and as-polished surfaces of GaAs wafers at room temperature is shown in Fig. IV-7. The strength of the as-polished surfaces after MOCVD is not dependent on test temperature. All values of strength after MOCVD are significantly smaller than those of the reverse side of the wafer which is as-cut (surface unchanged). Again the strength degradation may be the result from crack extension by thermal stresses during MOCVD.

The effect of soldering on the strength of the grid surface and metal backing surface was minimal, as seen in Fig. IV-8. The strength of the complete cell after soldered is controlled by the soldering metal alloy. The fracture-originating flaws of 20 X 40 mm GaAs samples subjected to four-point bending were found to be either a surface flaw or an edge flaw.

A typical fracture of a 20 X 40 mm GaAs wafer subjected to four-point bending is shown in Fig. IV-9(a). The fracture originating flaw of this sample was found to be a surface flaw, as indicated by an arrow. The area near the flaw is shown in Fig. IV-9(b) at a larger magnification.

The strength of brittle material $\sigma$ is related to the critical flaw size "a" as follows:

$$\sigma = \frac{K_{IC}}{Y\sqrt{a}} \qquad \text{(IV-6)}$$

where $K_{IC}$ is the fracture toughness. For GaAs, $K_{IC}$ values were determined in Section III of this report, and Y is the flaw shape factor.

More tests are required to determine the nature and the source of the fracture-originating flaws of GaAs cells as a function of cell processing.

The effect of cell processing on the fracture strength of 20 X 20 mm square wafers was also evaluated by four-point twisting at room temperature as shown in Fig. IV-10. The data presents all the testing results of each type of sample loaded both at corners and edges. No statistically significant difference was found on measured strength between corner loading and edge loading and therefore, data are treated as a single family. Fig. IV-10 shows that no twisting strength changes occur as a result of MOCVD as compared to the blank wafers. This is in contrast to earlier results by four-point bending tests which showed a decrease in strength after MOCVD. The twisting strength of the cells after metallization and solder application increases appreciably. This is consistent with earlier results by four-point bending tests and implies that any change in flaws is uniform from surface to

Figure IV-9. Typical Fracture of a 2 x 4 cm GaAs Wafer

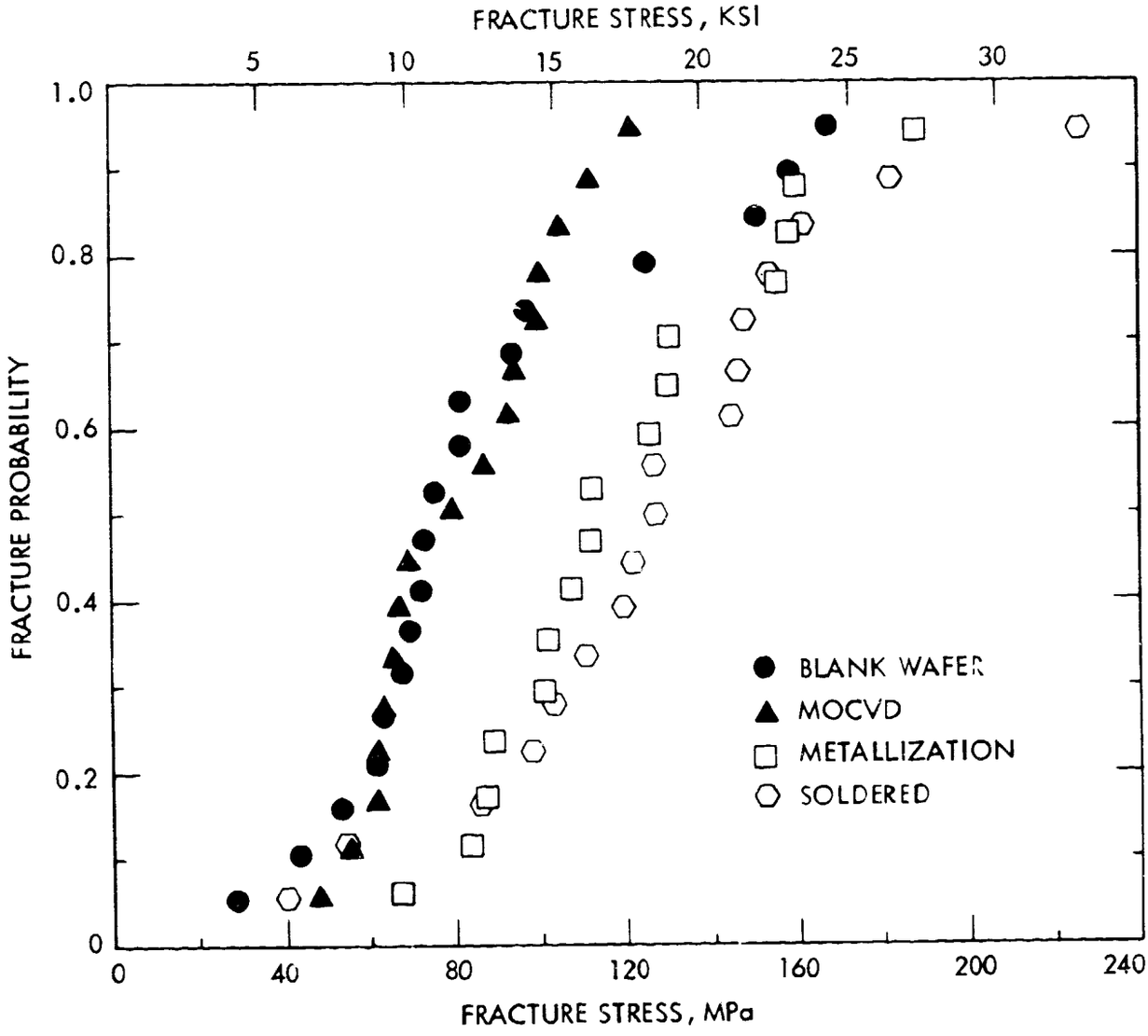


Figure IV-10. Effect of Cell Processing on the Fracture Strength of 2 x 2 cm GaAs Cells Tested by 4-Point Twisting at Room Temperature, Weibull Statistical Distribution Plot

edge. As discussed previously, the four-point twisting method is not only applying stresses on the sample surface but also at the sample edges. For a small sample, e.g., 20 X 20 mm wafers under twisting, the edge flaw extension under the transverse shear stresses (tearing) is the controlling factor for the fracture of square GaAs samples. Therefore, it can be concluded that MOCVD did not change the edge flaw configuration and thus no change in strength occurred. MOCVD appears to produce some wafer surface damage only.

b. Effect of Temperature

The effect of temperature on the measured strength of GaAs cells using four-point bending at several processing steps is shown in Fig. IV-6 to IV-8. As shown in Fig. IV-6 and IV-7, the effect of temperature on the strength of GaAs wafers was not observed within the temperature range -87 to 121°C.

A slight increase in the strength of soldered solar cells with decreasing temperature was found, as seen in Fig. IV-8. This observation is consistent with the strength of metals which usually increases with decreasing temperature.

c. Effect of Etch Pit Density (EPD)

The effect of etch pit density on the fracture strength of GaAs is shown in Fig. IV-11 and IV-12, for 20 X 20 mm and 20 X 40 mm samples. These preliminary data indicated that the strength of GaAs increases with increasing EPD values. A more detailed evaluation on the mechanism of alloy hardening/defect hardening in GaAs is required.

d. Strength of GaAs Wafers vs Silicon Wafers

A group of 10 silicon wafers, 20X20 mm, were also tested by four-point twisting for comparison.

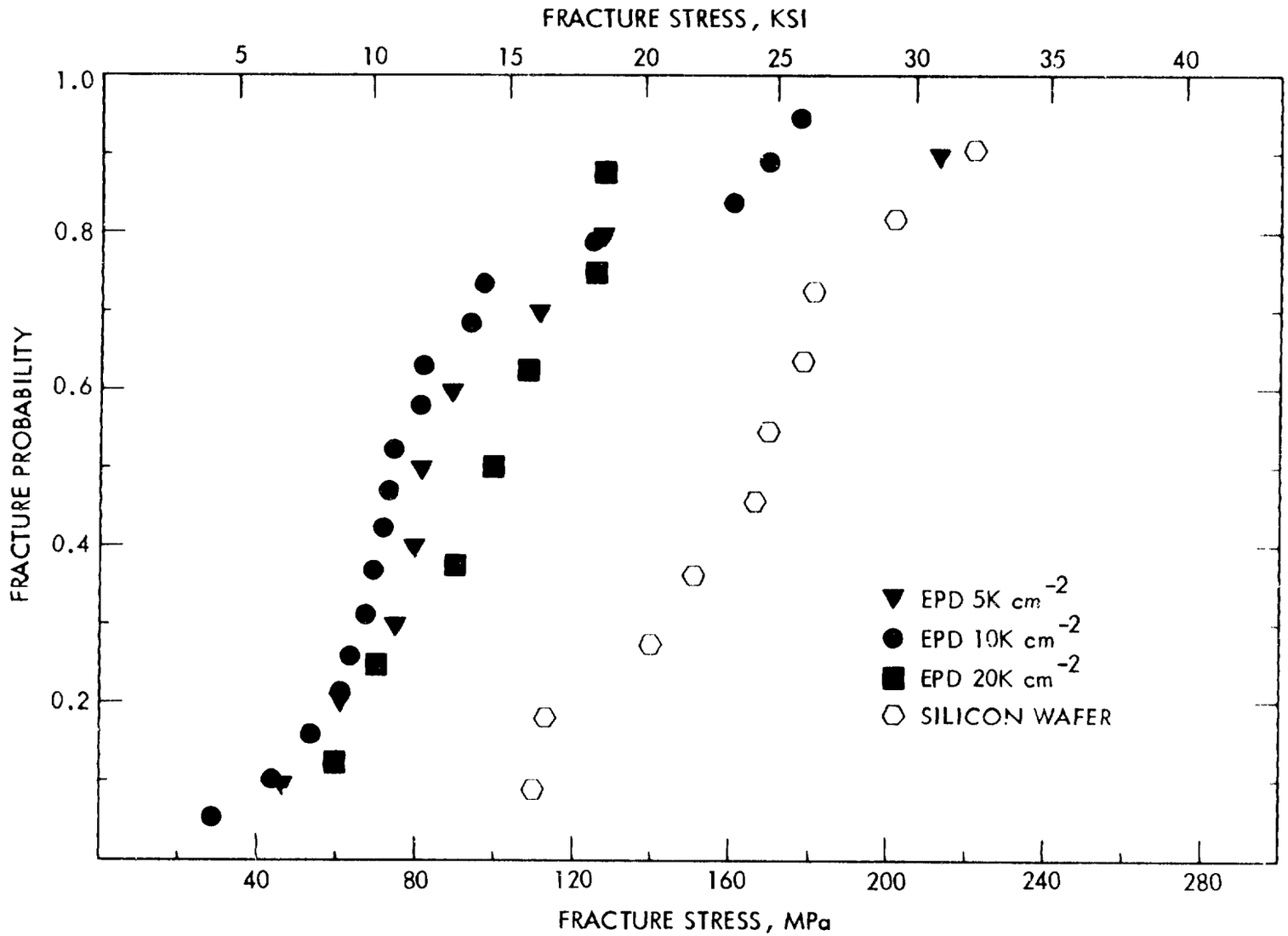


Figure IV-11. Effect of Etch Pit Density on the Fracture Strength of 2 x 2 cm GaAs Wafers Tested by 4-Point Twisting at Room Temperature, Weibull Distribution Plot

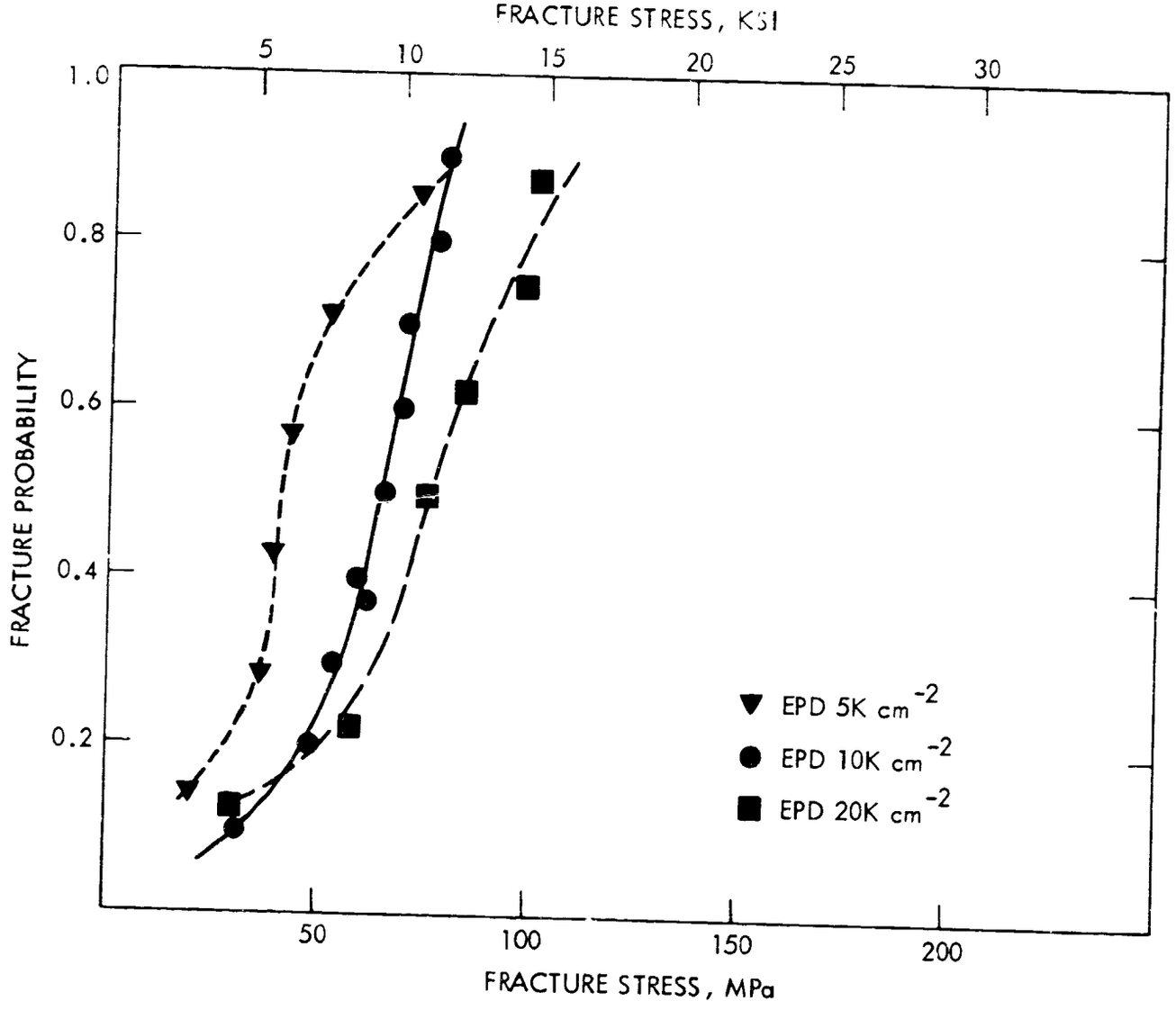


Figure IV-12. Effect of Etch Pit Density on the Modulus of Rupture of 2 x 4 cm GaAs Wafers' Polished Surface Tested at Room Temperature, Weibull Distribution Plot

These silicon samples were saw-cut from 50 mm (2 in.) diameter circular wafers. The material properties of these silicon wafers were given in Ref. 12. The fracture strength distribution of the silicon samples was also plotted in Fig. IV-11. It is found that the strength of GaAs at the 50% fracture probability is less than one-half that of silicon. This result is consistent with that found from the fracture toughness measurement in Sec. III of this report since the edge conditions of both GaAs and silicon wafers were similar, as-cut.

## D. CONCLUSIONS

1. MOCVD appears to produce some wafer surface damage which may be the result of the thermal shock during vapor deposition. Wafer edge damage was not observed. The thermal shock property of GaAs may be of interest.

2. AR coating and soldering materials increase the apparent st ength of cells.

3. Mechanical polishing does not produce a significant impr vement in the strength of the as-cut wafer.

4. The effect of temperature on the strength of GaAs wafers was not observed within the temperature range -87 to 121°C.

5. The preliminary results indicated that the strength of GaAs increases slightly with increasing EPD values. A more detailed evaluation on the mechanism of defect hardening/softening in GaAs is required.

6. The Weibull distribution plot of strength data is useful to describe the strength characteristics of wafers or cells and to describe the flaw distribution of each sample.

7. A long tail at the low-stress portion of the strength distribution curve was found for several types of samples. The wafers or cells in the low strength distribution are likely to be fractured during subsequent cell processing and handling. A proof test would be useful to eliminate these weak samples.

SECTION V

## RECOMMENDATIONS

The information presented in this report is the result of work carried out during the first phase of a research effort to generate a data base of mechanical and fracture property data for single crystal GaAs. The recommendations that follow are for the future work to generate additional information important for engineering design use. The recommendations are:

1. Evaluate the subcritical crack growth property of GaAs.

2. Determine the corrosion and erosion properties of GaAs as a function of fluid environments. This information is useful to improve the wafering process to produce thinner wafers with less surface damage at greater slicing speed.

3. Characterize the nature and origin of critical flaws in GaAs cells as a function of cell processing.

4. Determine the thermal shock behavior of crystalline GaAs.

5. Evaluate the feasibility of mechanical proof testing to eliminate weak wafers prior to cell processing.

6. Perform high temperature deformation tests to evaluate the mechanism of plastic deformation and fracture as a function of alloy hardening and defects (e.g., dislocations).

## REFERENCES


1. J. S. Blakemore, "Semiconducting and Other Major Properties of Gallium Arsenide" - J. Appl. Phys. 53(10), pp R123-R181, Oct. 1982.

2. "Standard Test Method for Young's Modulus, Shear Modulus and Poisson's Ratio for Glass and Glass-Ceramics by Resonance," ASTM C623-71, Am. Soc. Testing Mat'ls., Philadelphia, PA.

3. S. Spinner and W. E. Tefft, "A Method for Determining Mechanical Resonance Frequencies and for Calculating Elastic Moduli from These Frequencies", Proceeding, Am. Soc. Testing Mat'ls., ASTEA, pp 1221-1238, 1961.

4. R. F. S. Hearmon, "The Elastic Constants of Anisotropic Materials", Reviews of Modern Physics, Vol. 18, No. 3, pp 409-440, July 1946.

5. H. B. Huntington, "Ultrasonic Measurements on Single Crystals," Physical Review, Vol. 72, No. 4, pp 321-331, August 1947.

6. J. J. Wortman and R. A. Evans, "Young's Modulus, Shear Modulus, and Poisson's Ratio in Silicon and Germanium," J. Appl. Phys., 36(1), pp 153-156, Jan. 1965.

7. J. J. Petrovic, L. A. Jacobson, P. K. Talty, and A. K. Vasudevan, "Controlled Surface Flaws in Hot-Pressed $Si_3N_4$," J. Am. Ceram. Soc., 58 (3-4), 113-16 (1975).

8. C. P. Chen and M. H. Leipold, "Fracture Toughness of Silicon", Am. Ceram. Soc. Bulletin, 59(4), 469-472 (1980).

9. C. P. Chen, "Fracture Strength of Silicon Solar Cells", JPL/DOE Low-Cost Solar Array Project Report No. 5101-137, JPL Publication No. 79-102, Oct. 15, 1979.

10. W. Weibull, "A Statistical Distribution Function of Wide Applicability", J. Appl. Mech., Vol. 18, pp 293-297 (1951).

11. C. P. Chen and S-Y. S. Hsu, "Acoustic Emission Monitoring Crack Propagation in Single Crystal Silicon", Proceedings of Symposium of The Review of Progress in Quantitative Non-Destructive Evaluation, held at University of California-San Diego, La Jolla, CA. July 8-13, 1984.

12. C. P. Chen, M. H. Leipold and R. G. Ross, "Mechanical Proof Testing in Cell Processing", Proceedings of the Symposium, 17th IEEE Photovoltaic Specialists Conference, Kissimmee, FL., April 30-May 4, 1984.

END

DATE

FILMED

JUN 6 1985